



Advanced Magnetic Resonance Imaging in Pediatric Glioblastomas

Fabício Guimarães Gonçalves^{1*}, Angela N. Viaene^{2,3} and Arastoo Vossough^{1,4}

¹ Division of Neuroradiology, Department of Radiology, Children's Hospital of Philadelphia, Philadelphia, PA, United States,

² Department of Pathology and Laboratory Medicine, Children's Hospital of Philadelphia, Philadelphia, PA, United States,

³ Department of Pathology and Laboratory Medicine, Perelman School of Medicine, University of Pennsylvania, Philadelphia, PA, United States, ⁴ Department of Radiology, Perelman School of Medicine, University of Pennsylvania, Philadelphia, PA, United States

OPEN ACCESS

Edited by:

Manoj Kumar,
National Institute of Mental Health and
Neurosciences (NIMHANS), India

Reviewed by:

Santosh Kumar Yadav,
Sidra Medicine, Qatar
Hans-Georg Wirsching,
University Hospital Zürich, Switzerland
Manabu Natsumeda,
Niigata University, Japan
Timothy Richardson,
The University of Texas Health Science
Center at San Antonio, United States

*Correspondence:

Fabício Guimarães Gonçalves
goncalves.neuroradio@gmail.com

Specialty section:

This article was submitted to
Applied Neuroimaging,
a section of the journal
Frontiers in Neurology

Received: 30 June 2021

Accepted: 12 October 2021

Published: 10 November 2021

Citation:

Gonçalves FG, Viaene AN and
Vossough A (2021) Advanced
Magnetic Resonance Imaging in
Pediatric Glioblastomas.
Front. Neurol. 12:733323.
doi: 10.3389/fneur.2021.733323

The shortly upcoming 5th edition of the World Health Organization Classification of Tumors of the Central Nervous System is bringing extensive changes in the terminology of diffuse high-grade gliomas (DHGGs). Previously “glioblastoma,” as a descriptive entity, could have been applied to classify some tumors from the family of pediatric or adult DHGGs. However, now the term “glioblastoma” has been divested and is no longer applied to tumors in the family of pediatric types of DHGGs. As an entity, glioblastoma remains, however, in the family of adult types of diffuse gliomas under the insignia of “glioblastoma, IDH-wildtype.” Of note, glioblastomas still can be detected in children when glioblastoma, IDH-wildtype is found in this population, despite being much more common in adults. Despite the separation from the family of pediatric types of DHGGs, what was previously labeled as “pediatric glioblastomas” still remains with novel labels and as new entities. As a result of advances in molecular biology, most of the previously called “pediatric glioblastomas” are now classified in one of the four family members of pediatric types of DHGGs. In this review, the term glioblastoma is still apocryphally employed mainly due to its historical relevance and the paucity of recent literature dealing with the recently described new entities. Therefore, “glioblastoma” is used here as an umbrella term in the attempt to encompass multiple entities such as astrocytoma, IDH-mutant (grade 4); glioblastoma, IDH-wildtype; diffuse hemispheric glioma, H3 G34-mutant; diffuse pediatric-type high-grade glioma, H3-wildtype and IDH-wildtype; and high grade infant-type hemispheric glioma. Glioblastomas are highly aggressive neoplasms. They may arise anywhere in the developing central nervous system, including the spinal cord. Signs and symptoms are non-specific, typically of short duration, and usually derived from increased intracranial pressure or seizure. Localized symptoms may also occur. The standard of care of “pediatric glioblastomas” is not well-established, typically composed of surgery with maximal safe tumor resection. Subsequent chemoradiation is recommended if the patient is older than 3 years. If younger than 3 years, surgery is followed by chemotherapy. In general, “pediatric glioblastomas” also have a poor prognosis despite surgery and adjuvant therapy. Magnetic resonance imaging (MRI) is the imaging modality of choice for the evaluation of glioblastomas. In addition to the typical conventional MRI features, i.e., highly heterogeneous invasive masses with indistinct borders, mass effect on surrounding

structures, and a variable degree of enhancement, the lesions may show restricted diffusion in the solid components, hemorrhage, and increased perfusion, reflecting increased vascularity and angiogenesis. In addition, magnetic resonance spectroscopy has proven helpful in pre- and postsurgical evaluation. Lastly, we will refer to new MRI techniques, which have already been applied in evaluating adult glioblastomas, with promising results, yet not widely utilized in children.

Keywords: advanced MRI, children, conventional MRI, diffusion-weighted imaging, glioblastoma, magnetic resonance spectroscopy, perfusion weighted imaging

INTRODUCTION

This review was conceived and developed during a watershed moment, in which major changes are occurring in how brain tumors are classified. During the last few years, new concepts and entities have emerged, and well-known diagnoses and terminology have been abandoned. According to the shortly upcoming 5th edition of the World Health Organization Classification of Tumors of the Central Nervous System (CNS) (WHO/CNS/5), the term “glioblastoma” is no longer applicable for tumors in the family of pediatric types of diffuse high-grade gliomas (DHGGs) (1). Glioblastoma only remains, as an entity, in the family of adult types of diffuse gliomas (1).

As stated in the WHO/CNS/5, there are three components in the family of adult types of diffuse gliomas and four in the family of pediatric types of DHGG. The three adult types of diffuse gliomas are represented by the (1) astrocytoma, IDH-mutant (grades 2, 3, and 4); (2) oligodendroglioma, IDH-mutant, and 1p/19q-codeleted (grades 2 and 3) and (3) glioblastoma, IDH-wildtype (grade 4) (1). The four pediatric types of DHGGs (all grade 4 tumors) are represented by the (1) diffuse midline glioma, H3 K27-altered; (2) diffuse hemispheric glioma, H3 G34-mutant; (3) diffuse pediatric-type high-grade glioma, H3-wildtype and IDH-wildtype; and (4) infant-type hemispheric glioma (1). This review will focus on the pediatric types of DHGGs (except the diffuse midline glioma, H3 K27-altered) and the two grade 4 adult types of diffuse gliomas, namely the astrocytoma, IDH-mutant grade 4 (formerly known as glioblastoma, IDH-mutant), and the glioblastoma, IDH-wildtype (1). These two latter diffuse gliomas are typically found in adults, but can also occasionally occur in older children, particularly teenagers.

Despite the separation and removal of the term “glioblastoma” from the family of pediatric type DHGGs, as per the WHO/CNS/5 (1), this paper will still apocryphally employ the term due to a number reasons, including: (1) its preeminent historical relevance, (2) the bulk of the available neuro-oncology literature refers to it as glioblastoma, (3) the paucity of recent literature explicitly dealing with the most current classification (WHO/CNS/5), and (4) a convenient way to refer to grade 4 DHGGs that can occur in children, beyond the diffuse midline glioma, H3 K27-altered, and glioblastoma, IDH-wildtype, which may still be sometimes seen in the pediatric population.

Studies on glioblastomas in children are more limited in number than their adult counterparts, despite this tumor’s

clinical relevance and the substantial patient burden that accompanies this diagnosis. Even though “glioblastomas in children” share similar morphological characteristics to adult glioblastomas, they are much less common and present distinct gene expression and molecular profiles, explaining observed differences in adjuvant treatment response. Given their relative rarity, most of the available literature relies on studies involving small numbers of patients in the form of case reports and small case series. Fundamental concepts of pathology, clinical features, management, structural imaging, and advanced imaging techniques (some not widely available such as metabolic and physiologic magnetic resonance imaging) to study “glioblastomas in children” will be reviewed.

BACKGROUND

Glioblastomas are highly aggressive tumors whose cell of origin is not fully clarified. They are the most lethal and most common primary CNS neoplasm in adults, with incidence peak in the sixth and seventh decades (2). They are relatively rare in children, representing 0.6–7.9% of all “glioblastomas” (3), and accounting for 3–15% of all primary pediatric CNS tumors (4). They can occur at any age, more frequently around the second decade of life (4–6).

“Glioblastomas” may arise anywhere in the developing CNS. Their most common location is in the supratentorial compartment (7), occurring in 30–50% of the patients in the cerebral hemispheres (8). Involvement of deeper structures such as the thalamus, corpus callosum, and hypothalamus is less common (9). Spinal cord involvement is rare, representing only 3% of all cases (8). Very rarely “pediatric glioblastomas” may occur in the cerebellum (1–2% of all patients) (10).

Signs and Symptoms

Signs and symptoms are often non-specific, typically of short duration, and usually result from increased intracranial pressure (headache, behavior changes, early morning nausea/emesis, diplopia, papilledema, and altered sensorium) (4, 5, 11). In addition, localizing symptoms may occur, namely focal motor deficits, hemiplegia, pyramidal tract findings, dysmetria, and chorea (12). Infants and young children may also manifest ambiguously with failure to thrive, lethargy, and macrocephaly. Finally, precipitous neurological deterioration may also occur,

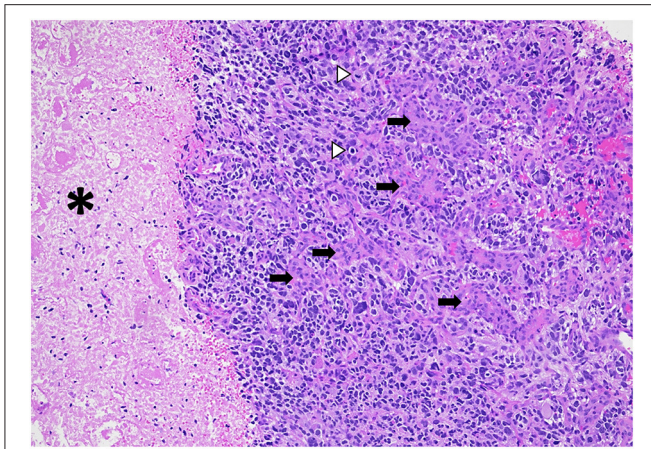


FIGURE 1 | Diffuse hemispheric glioblastoma, H3 G34 mutant (histologic “glioblastoma”) demonstrating high cellularity, nuclear pleomorphism, microvascular proliferation (arrows), necrosis (asterisks), and mitotic figures (arrowheads). HandE stain, 100x magnification.

commonly from intratumoral hemorrhage or seizures (9). Seizures may be present in around 30% of affected children, more commonly when lesions are superficially located in the frontal or temporal lobes (5, 11, 13).

Pathology and Molecular Diagnosis

“Glioblastomas” are typically large, highly vascularized, heterogeneous, and infiltrative masses, and often have irregular margins. On gross pathology, the peripheral rims are pink-gray and solid and may contain a yellow, soft necrotic center, and often contain hemorrhagic foci (14). Microscopically, they typically show increased cellularity, high mitotic activity, pleomorphic cells, microvascular proliferation, and necrosis (**Figure 1**). There are no gross or microscopic histologic differences between “glioblastomas” affecting adults or children (15–17); however, certain histologic subtypes may be more frequently encountered in specific age groups.

Their diffusely infiltrative behavior is characteristic, typically showing hypercellularity, nuclear atypia, necrosis (which may be pseudopalisading), and vascular endothelial cell proliferation. Glioblastomas are friable and highly vascularized masses in which thrombosed vessels, bleeding, and necrosis can be identified (18). Calcification is atypical but can be seen in radiation-associated “secondary glioblastomas.” Radiation-associated “secondary glioblastomas” may be observed many years following CNS radiation treatment for childhood malignancies, including leukemia and other brain tumors such as medulloblastomas and ependymomas (**Figure 2**) (18). However, radiation-associated “secondary glioblastomas” are uncommon, with an average time to develop around 9 years (18). Contrary to adult patients, the progression of low-grade gliomas into “secondary glioblastoma” is very rare in children.

Traditionally, glioblastomas have been histologically classified as giant-cell glioblastoma, gliosarcoma, and epithelioid glioblastoma (19). Epithelioid “glioblastomas” are known to be more common in children and are characterized by large

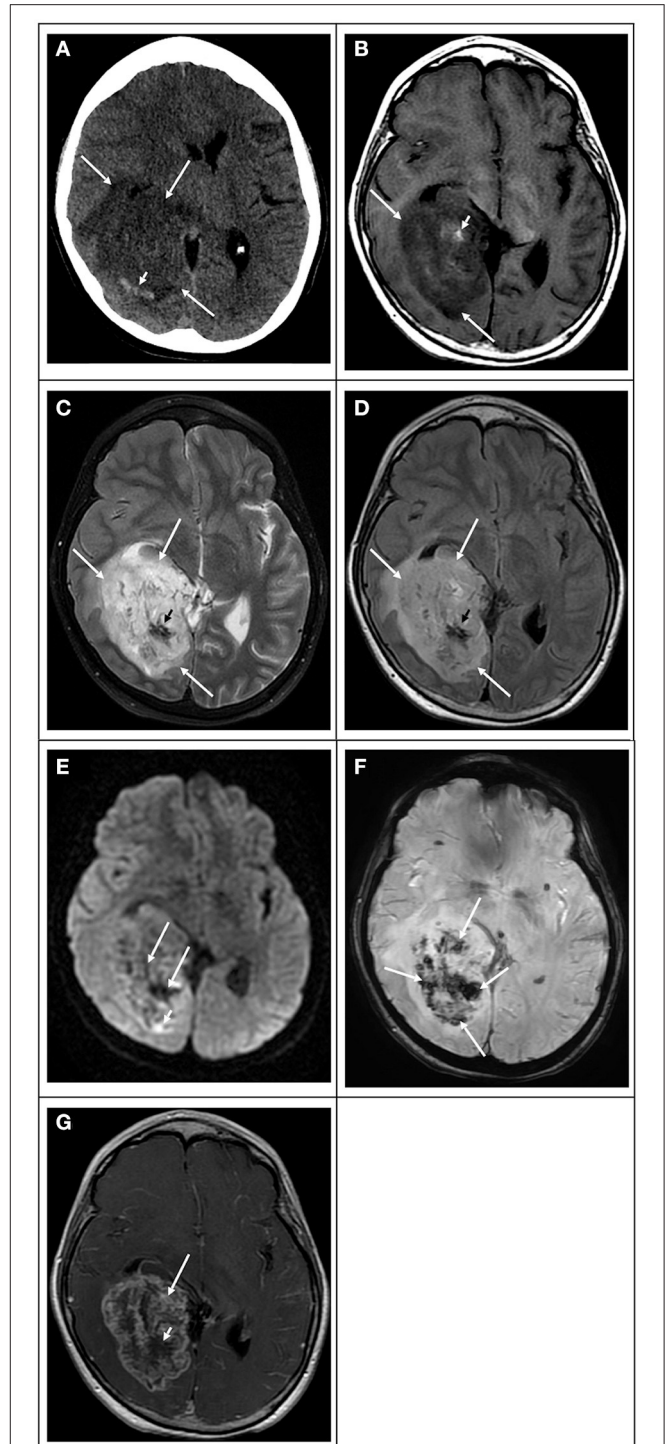


FIGURE 2 | Radiation-induced secondary “glioblastoma” in a 17-year-old girl who had a previous posterior fossa ependymoma at age 5. **(A)** Computed tomography image in the axial plane shows a large ill-defined tumor in the right temporal and occipital lobes (white arrows), causing mass effect, compression of the right lateral ventricle, and midline deviation. The lesion is associated with vasogenic edema and hemorrhage (white arrowhead). **(B)** T1 weighted image in the axial plane shows that the bulk of the lesion is hypointense (white arrows) with scattered hyperintensity foci due to intratumoral hemorrhage

(Continued)

FIGURE 2 | (white arrowhead). **(C)** T2 weighted image and **(D)** FLAIR image in the axial plane show that the bulk of the lesion is hyperintense with scattered hypointense foci due to intratumoral hemorrhage. **(E)** Diffusion-weighted image in the axial plane shows that the lesion is heterogeneous in signal. The bulk of the lesion is isointense to the normal brain parenchyma with scattered hyperintense foci due to intratumoral hemorrhage and small peripheral hyperintense foci (white arrowhead), which had lower values on the ADC maps (not shown) in keeping with restricted diffusion. **(F)** Susceptibility weighted image in the axial plane shows extensive signal drop within the tumoral bed (white arrows) in keeping with diffuse hemorrhage. **(G)** T1-weighted contrast-enhanced image in the axial plane shows that the tumor enhances heterogeneously. The mass has avid enhancement with central non-enhancing areas in keeping with necrotic tissue.

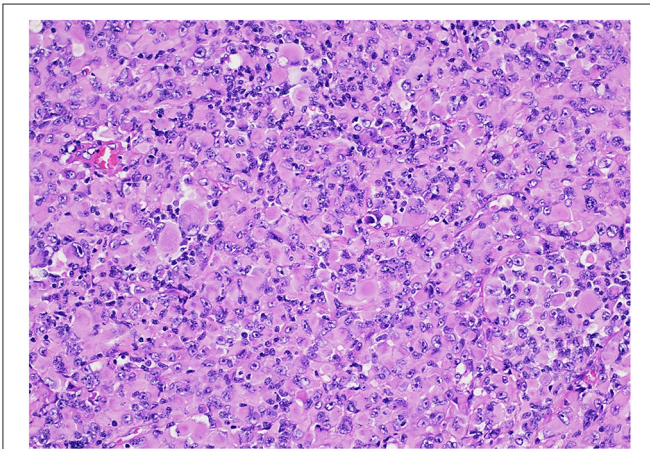


FIGURE 3 | Diffuse pediatric-type high-grade glioma, H3-wildtype and IDH-wildtype (“histologic epithelioid glioblastoma”) characterized by sheets of tumor cells with distinct nuclear borders, a moderate to large amount of eosinophilic cytoplasm, eccentrically-located nuclei, and prominent nucleoli. HandE stain, 200x magnification.

eosinophilic cells, prominent melanoma-like nuclei, and often rhabdoid cells (**Figure 3**) (9). However, in the WHO/CNS/5, subtypes are not listed in the classification, but are further discussed in their respective chapters (1).

Many high-grade gliomas (HGGs) have also more recently been classified and diagnosed by methylation profiling, and entities once thought to comprise “pediatric glioblastomas” have been reclassified as other entities and vice versa. In addition, molecular features may vary by location. For example, what was thought to be a uniform group of glioblastomas occurring in the posterior fossa, now comprises distinct molecular entities (based on methylation profiles), namely anaplastic astrocytoma with piloid features; glioblastoma, IDH wildtype; diffuse midline glioma H3 K27M mutant; and astrocytoma, IDH mutant (20).

Previously, CNS tumor grading fundamentally relied on histological features with rare exceptions (i.e., diffuse midline glioma, H3K27M-mutant). Currently, specific molecular markers also play a major role in diagnosis and prognosis and even in assignment of tumor grade. The WHO/CNS/5 has combined histological and molecular grading, meaning that molecular parameters have now been added as biomarkers

of grading and can sometimes upgrade a lesion, despite its conventional histology characteristics (1).

Formerly, glioblastomas have been classified, based on the isocitrate dehydrogenase (IDH) gene mutation status, into three major subgroups: IDH-wildtype (the majority of the patients), IDH-mutant, and not otherwise specified (19, 21). “IDH-mutant glioblastomas” were often considered secondary neoplasms (i.e., progressed from lower-grade IDH-mutant astrocytomas), while IDH-wildtype glioblastomas typically represented *de novo* neoplasms, mainly in older adults (9).

According to WHO/CNS/5, glioblastomas, as valid entities, are, by definition, only represented by the IDH-wildtype. They may also incorporate three genetic parameters, namely TERT promoter mutation, EGFR gene amplification, the combined gain of entire chromosome 7, and loss of entire chromosome 10 [+7/−10] (1). Therefore, the presence of one or more of the latter three in a patient with IDH-wildtype diffuse astrocytic tumor suffices to assign the highest WHO grade (1). In the family of adult diffuse gliomas, the tumors that do not show microvascular proliferation or necrosis, but show either TERT promoter mutation, EGFR mutation, or +7/-10 chromosome copy number changes will still be classified as glioblastoma when considering the integrated diagnosis (1). In other words, even though there may not be full histologic features of “glioblastoma” in these diffuse gliomas, the addition of specific molecular information may still classify them as glioblastoma. Note that occasionally, adult type glioblastoma, IDH-wild type may be seen in older children.

At present, the WHO/CNS/5 (1) recognizes three adult types of diffuse gliomas, namely:

- 1) Astrocytoma, IDH-mutant
- 2) Oligodendroglioma, IDH-mutant, and 1p/19q-codeleted and the
- 3) Glioblastoma, IDH-wildtype.

Astrocytomas, IDH-mutant, can be classified in grades 2, 3, or 4 (formerly IDH-mutant glioblastoma) (1). Notably, the term “glioblastoma” is no longer valid in the setting of a pediatric type diffuse glioma (1). In addition, the WHO/CNS/5 (1) endorses four pediatric types of DHHGs, namely:

- 1) Diffuse midline glioma, H3 K27-altered
- 2) Diffuse hemispheric glioma, H3 G34-mutant
- 3) Diffuse pediatric-type high-grade glioma, H3-wildtype and IDH-wildtype
- 4) Infant-type hemispheric glioma.

The characteristically altered genes and molecular profiles in each of the four pediatric types of DHHGs are (1):

- 1) Diffuse midline glioma, H3 K27-altered: H3 K27, TP53, ACVR1, PDGFRA, EGFR, EZHIP
- 2) Diffuse hemispheric glioma, H3 G34-mutant: H3 G34, TP53 (**Figure 4**), ATRX
- 3) Diffuse pediatric-type high-grade glioma, H3-wildtype, and IDH-wildtype: IDH-wildtype, H3-wildtype, PDGFRA, MYCN, EGFR (methylome)

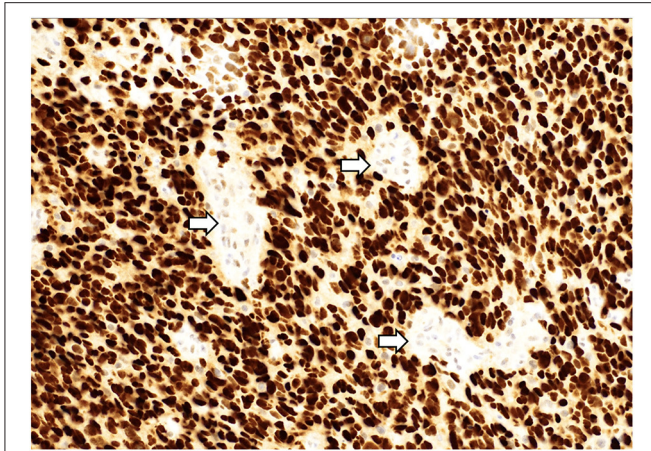


FIGURE 4 | A “glioblastoma” with a mutation in TP53 demonstrating strong, diffuse nuclear staining for p53 with wildtype staining present in vessels (arrows). p53 immunostain, 200x magnification.

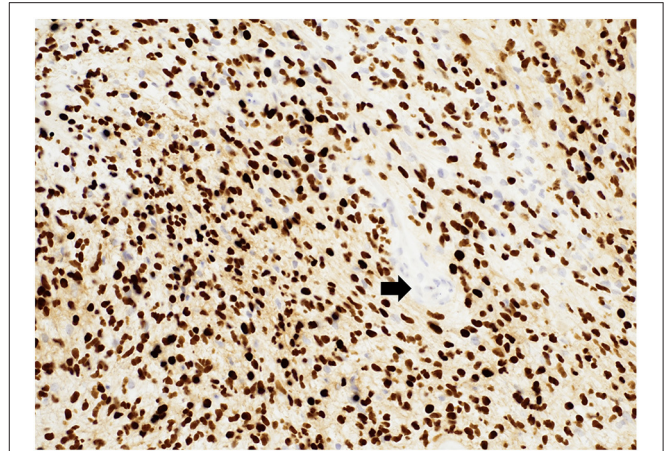


FIGURE 5 | Diffuse midline glioma, H3K27M-altered demonstrating diffuse nuclear staining for H3K27M with negative endothelial cells serving as an internal control (arrow). H3K27M immunostain, 200x magnification.

4) Infant-type hemispheric glioma: NTRK family, ALK, ROS, MET.

Lack of IDH mutation is known to impact therapy outcomes negatively in adult patients. “Glioblastomas in children” and other HGG typically demonstrate a low incidence of IDH mutation (seen in ~6% of all pediatric HGGs), and such alterations are infrequent in younger children (22). Therefore, the majority of true glioblastomas in children are thought to be IDH-wildtype. The incidence of IDH-mutant or “secondary glioblastomas” may be higher in older adolescents and younger adults (23).

Mutations in histone genes are the most common molecular findings in pediatric HGGs with H3 K27M mutations associated with midline tumors (**Figures 5, 6**) and H3 p.G34R/V mutations occurring in hemispheric tumors. The majority of these tumors are histologically high-grade; however, it should be noted that infiltrative, astrocytic tumors of the midline with H3 K27M mutations are classified as “diffuse midline gliomas,” and regardless of histologic grade, correspond to WHO grade 4 (19). In addition, co-occurring mutations in TP53 (**Figure 4**) and ATRX (**Figure 7**) may be seen in tumors with H3 mutations, whereas IDH mutations are not observed (24, 25). Of note, circumscribed/non-diffuse gliomas of the midline are not considered grade 4, according to the (WHO/CNS/5) (26). Diffuse midline gliomas are not the primary focus of this paper.

Diffuse midline gliomas are one of the most severe pediatric brain tumors, with dismal prognosis despite developments in diagnosis and therapeutics. According to Castel et al. (27) there are two subgroups of diffuse midline gliomas, H3-K27M-mutant, namely H3.1-K27M and H3.3-K27M with differences in prognosis and phenotypes. According to them, the differences between H3.1/H3.3 subgroups may be a result of distinct cells of origin or due to the type of histone mutated. In their study they found that the type of histone H3 mutated could also predict the outcome of DIPG patients more efficiently than

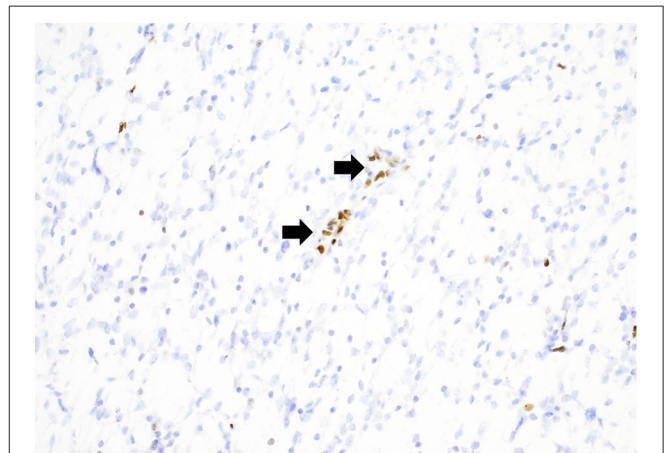


FIGURE 6 | Diffuse midline glioma, H3K27-altered demonstrating a loss of nuclear staining for H3K27me3 with positive endothelial cells serving as an internal control (arrows). H3K27me3 immunostain, 200x magnification.

clinical and radiological characteristics of the tumors (27). An in depth discussion about diffuse midline gliomas was not included here because of their complexity and specificities and due to space limitations, being necessary a specific paper to discuss them accordingly.

“Pediatric glioblastomas” commonly have a higher incidence of p53 mutation/overexpression (particularly in children <3 years) than mutation of epithelial growth factor receptor (EGFR) or deletion of phosphatase and tensin homolog (PTEN), which are common features of “adult glioblastomas” (9). In addition, ATRX mutations (**Figure 7**) have been reported in a fraction of “pediatric glioblastomas,” usually associated with other mutations (28). Vascular endothelial growth factor (VEGF) is commonly expressed by “adult glioblastomas” and is responsible for increased vascularity, tumor progression, and infiltration. Therefore, anti-VEGF (bevacizumab) therapy is frequently

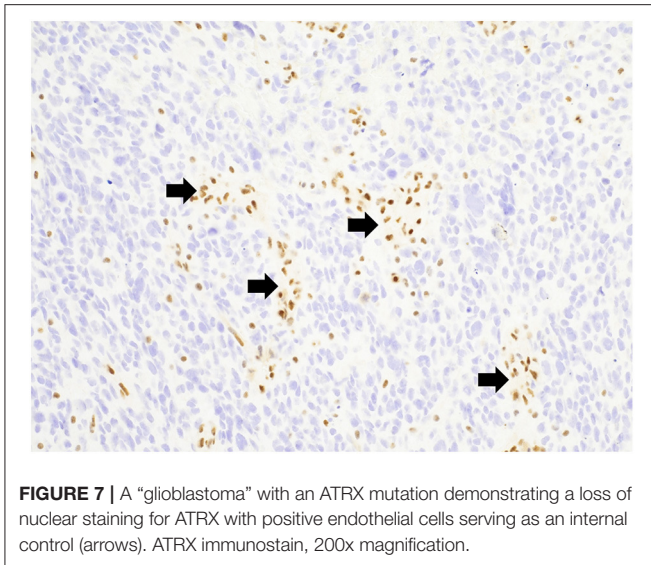


FIGURE 7 | A “glioblastoma” with an ATRX mutation demonstrating a loss of nuclear staining for ATRX with positive endothelial cells serving as an internal control (arrows). ATRX immunostain, 200x magnification.

employed in “adult glioblastomas.” However, VEGF expression is relatively infrequent in “pediatric glioblastomas,” which may explain the comparative ineffectiveness of anti-VEGF therapy in children (29).

The mechanism of action of temozolomide (TMZ), one of the chemotherapy agents to treat glioblastomas, is by promoting DNA methylation. On the other hand, O⁶-Methylguanine-DNA Methyltransferase (MGMT) is a DNA repair enzyme, rescuing neoplastic cells from alkylating agent-induced damage. Therefore, MGMT activation leads to increased resistance to chemotherapy with alkylating agents. MGMT promoter methylation status has crucial prognostic importance in glioblastomas. Inactivation of MGMT generally correlates with chemotherapy responsiveness (30) and increased median event-free survival (31). Studies on MGMT expression in “pediatric glioblastomas” have demonstrated little alteration in the methylation promoter status in children, which may explain the reduced efficacy of TMZ in children compared to adults (32). Regarding the diffuse midline gliomas, H3 K27M mutant, MGMT promoter is unmethylated in almost all cases, which explains the failure of clinical trials administering TMZ to patients with this diagnosis (33, 34). Whenever present, the prognostic significance of inactivating hypermethylation of MGMT confers a survival benefit to affected children.

NEUROIMAGING

Computed Tomography

Computed tomography (CT) may be the first imaging modality in children to detect an intracranial neoplasm. On CT, “pediatric glioblastomas” typically present as poorly margined heterogeneous lesions with mass effect and variable areas of hyperattenuation, which may be partially due to hemorrhage (Figure 8). Areas of hypoattenuation may correspond to necrosis or surrounding edema. Contrast-enhanced CT features are

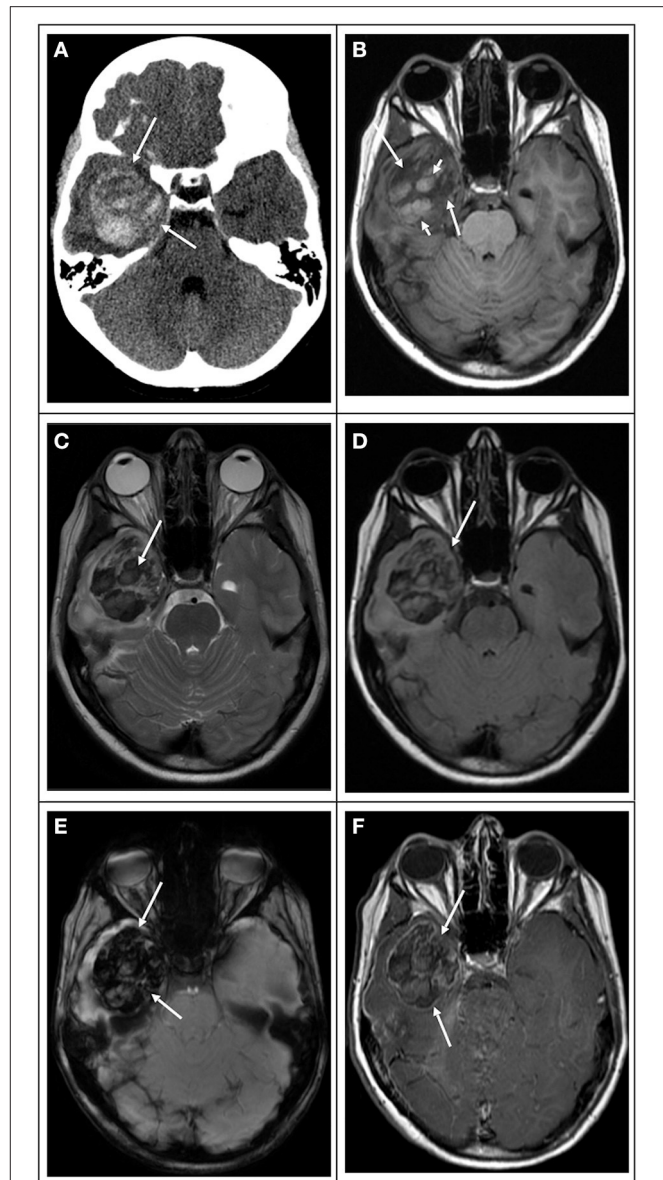


FIGURE 8 | 10-year-old male with worsening headaches and papilledema due to a right temporal lobe “glioblastoma”. **(A)** Computed tomography image in the axial plane shows a heterogeneously hyperdense area in the right temporal lobe in keeping with a diffusely hemorrhagic lesion. At this point, the differential includes vascular lesions or tumors. **(B)** T1 weighted image in the axial plane shows that the lesion is heterogeneous with mixed signals. The tumoral bed is hypointense (white arrows) with scattered hyperintensity components due to intratumoral hemorrhage (white arrowheads). **(C)** T2 weighted image and **(D)** FLAIR images in the axial plane show that the bulk of the lesion is hypointense due to diffuse intratumoral hemorrhage. **(E)** Susceptibility weighted image in the axial plane shows extensive signal drop within the tumoral bed (white arrows) in keeping with diffuse hemorrhage. **(F)** T1-weighted contrast-enhanced image in the axial plane shows that the tumor enhances heterogeneously. The mass has thin peripheral enhancement (arrowhead) with internal variable minimal enhancement due to hemorrhage and necrosis.

variable, ranging from minor to marked enhancement and from solid to heterogeneous enhancement. Necrotic lesions may show rim enhancement, typically with irregular borders (35). Typical

TABLE 1 | Typical computed tomography and magnetic resonance imaging features of pediatric glioblastomas.

Imaging features	
Generalities	<ul style="list-style-type: none"> - Variable size (typically large) - Poorly marginated - Heterogeneous - Mass effect - Variable hemorrhage - Variable vasogenic edema
Location	<ul style="list-style-type: none"> - Cerebral hemispheres (most common) - Brainstem - Cerebellum - Spinal cord
Computed tomography	
Non-enhanced	<ul style="list-style-type: none"> - Variable areas of hyperattenuation (hemorrhage/hypercellularity) - Hypoattenuation → necrosis or surrounding edema
Contrast enhanced	<ul style="list-style-type: none"> - Variable enhancement <ul style="list-style-type: none"> - Minor to marked - Solid to heterogeneous - Necrotic lesions may present ring enhancement
Magnetic resonance imaging	
T1WI	<ul style="list-style-type: none"> - Iso- to hypointense (relative to gray matter) - Edema and necrosis → Hypointense
T2WI	<ul style="list-style-type: none"> - Hyperintense (relative to gray matter) - Variable vasogenic edema → hyperintense
FLAIR	<ul style="list-style-type: none"> - Hyperintense (relative to gray matter) - Variable vasogenic edema → hyperintense
Contrast enhanced T1WI	<ul style="list-style-type: none"> - Variable - Complex - Thick irregular rim (typical) - No enhancement (rare)
Susceptibility weighted imaging and T2* weighted imaging	<ul style="list-style-type: none"> - When neoplasms are complicated by hemorrhage → low signal
Diffusion weighted imaging	<ul style="list-style-type: none"> - Variable restricted diffusion - Restricted diffusion (typical in solid areas)
Dynamic susceptibility contrast	<ul style="list-style-type: none"> - ↑ CBV
Dynamic contrast-enhanced	<ul style="list-style-type: none"> - ↑ K^{trans} - ↑ K^{ep} - ↑ V_e - ↑ CBV - ↑ CBF
Arterial spin labeling	<ul style="list-style-type: none"> - ↑ CBF
Proton 1/H Magnetic resonance spectroscopy	<ul style="list-style-type: none"> - ↑ Choline - ↓ NAA - ↑ Lactate

T1WI, T1 Weighted imaging/T2WI, T2 Weighted Imaging. ↑, high; ↓, low; →, resulting in.

CT findings of “pediatric glioblastomas” can be seen in the **Table 1**.

Magnetic Resonance Imaging

Magnetic Resonance Imaging (MRI) is the imaging modality of choice in the evaluation of “pediatric glioblastomas.” It delivers superior spatial and contrast resolution, allowing improved non-invasive assessment of the tumor and surrounding brain, and

helps with neurosurgical and radiation planning (36). MRI findings of “pediatric glioblastomas” are not specific. Masses are typically heterogeneous with indistinct margins, mass effect on surrounding structures, and a variable degree of enhancement (complex, variable, or rarely absent). Relative to gray matter, “pediatric glioblastomas” may demonstrate iso- to hypointense T1 signal and heterogeneously hyperintense T2 signal with surrounding edema, which is readily evident on fluid attenuation inversion recovery (FLAIR) images (35, 37). When the neoplasms are complicated by hemorrhage, different signal characteristics can be seen, such as T1 hyperintense, T2 hypointense, low signal on T2*, and susceptibility-weighted imaging. Typical conventional MRI features of “pediatric glioblastomas” can be seen in the **Table 1**.

A distinction must be made between contrast enhancement and increased perfusion. The degree and extent of contrast enhancement reflect pathologic changes of the blood-brain barrier and extravascular leakage of contrast (38, 39). The blood-brain barrier breakdown can result from the destruction of normal capillaries by a neoplastic process or from the pathologic structure of the vascular walls of newly formed abnormal capillaries. The degree of perfusion reflects tumor vascularity, which may or may not be associated with blood-brain barrier breakdown (38, 39).

“Pediatric glioblastomas” are known to be less common than adult glioblastomas. As stated previously, there are no gross and microscopic pathology differences between adult and pediatric glioblastomas. However, there are major molecular and genetic differences between, which is unequivocally demonstrated and established by the WHO/CNS/5. In addition, these tumors also differ in terms of cause-specific survival and overall survival (9).

Literature comparing imaging differences between adult and pediatric glioblastomas is very scarce. Both tumors are typically heterogeneous and may demonstrate mass effect, vasogenic edema, restricted diffusion, and contrast enhancement. “Pediatric glioblastomas” may present as masses with more solid enhancement, whereas adult glioblastomas have a higher tendency to be necrotic, and therefore more commonly present as rim enhancing lesions.

Advanced MRI Neuroimaging

The number of studies and evidence supporting the utility of advanced MRI neuroimaging techniques in children is much more limited than in adult glioblastomas, but the general principles similarly apply. Most of the literature on advanced MRI neuroimaging techniques in children is with limited affirmed clinical validation if analyzed in isolation. Thus, these techniques should be applied in conjunction with conventional imaging, under a multiparametric approach, for the imaging evaluation of brain tumor diagnosis and follow-up.

Diffusion-Weighted Imaging

Diffusion-weighted imaging (DWI) is a well-known clinical imaging technique applied in the study of brain tumors. However, there are very few studies dedicated specifically to using diffusion-weighted imaging (DWI) and apparent diffusion coefficient (ADC) measurements in assessing “pediatric

glioblastomas.” DWI is a superb technique that measures the degree of movement of water molecules and probes their relation to the surrounding environment in both the normal and diseased states. Quantitative DWI information on the extent of the movement of water molecules can be obtained by the apparent ADC calculation (40, 41).

DWI is a mainstay in routine brain tumor MRI, typically acquired with two b -values for ADC calculation ($b = 0$ and $b = 1,000$ s/mm²). DWI is very helpful in pointing toward the diagnosis, providing information regarding tumor grade and type, and monitoring treatment response (42). In addition, several authors have shown that the different components of the tumors, surrounding edema, and normal surrounding white matter may have distinct ADC values (40, 43–45).

Several authors have demonstrated the utility of DWI in the differential diagnosis of cystic masses (46–49). Cystic and necrotic components of a tumor have higher ADC values, reflecting the increased water movement characterizing these components. Enhancing components of HGGs typically show lower ADC values than non-enhancing tumor and peritumoral edema (40). DWI often demonstrates restricted (reduced) diffusion (low ADC values) in solid portions of HGGs, in keeping with high cellular density and/or high nuclear-to-cytoplasm ratios (50). Restricted diffusion can be observed in some gliomas, notably higher grade tumors such as anaplastic astrocytomas, glioblastomas, diffuse midline gliomas, and anaplastic ependymomas.

DWI has been used to distinguish areas of peritumoral neoplastic cell infiltration from peritumoral edema, a critical distinction when dealing with HGGs (40). In addition, ADC values can be used to distinguish normal white matter from necrotic or cystic areas, edema, and solid-enhancing tumors (51). However, the distinction between infiltrating tumors from edema or nearby normal-appearing brain is sometimes inaccurate in glioblastoma, as small amounts of infiltrating tumor cells may be present in these areas, but not in enough quantities to significantly alter the diffusion parameters. DWI may also aid in the differentiation of abscesses from necrotic or cystic brain tumors such as HGGs (52, 53).

ADC is negatively correlated with cell proliferation indices such as Ki-67 (54). The signal characteristics on DWI and ADC maps can be strongly correlated to grade in pediatric brain tumors, and they may assist with preoperative diagnostic predictions (55). In addition, ADC measurements can be used to differentiate between HGGs from low-grade gliomas. Wang et al. (56), in a recent meta-analysis including 1,172 patients, found an area under the curve (AUC) for b values of 1,000 and 3,000 s/mm² to be of 0.91 and 0.92, respectively. Their results demonstrated that ADC measurements had high diagnostic performance in discriminating HGGs from low-grade gliomas.

A study by Chang et al. (35) involving 11 patients with glioblastomas found that the DWI signal intensity in the solid portion of the tumor was hyperintense compared to the white matter. The ADC values for the solid tumor component ranged from 0.53 to 1.30×10^{-3} mm²/s (mean, $1.011 \pm 0.29 \times 10^{-3}$ mm²/s) and for white matter from 0.60 to 0.98×10^{-3} mm²/s (mean, $0.824 \pm 0.130 \times 10^{-3}$ mm²/s). In one of the patients,

a recurrent glioblastoma demonstrated increased DWI signal in the tumoral bed months after total gross removal of the tumor (35). Tumor recurrence has been reported to have significantly lower ADC values than radiation necrosis (57, 58). DWI and ADC calculation may be utilized as a surrogate marker for monitoring the response of tumor therapy (59, 60). For example, Chenevert et al. (59) found a rapid increase in the mean ADC values shortly after treatment initiation, and the magnitude of the diffusion changes corresponded with clinical outcome.

Most published experience in applying DWI in pediatric tumors has focused mainly on posterior fossa tumors. Higher ADC values at the baseline have been reported to have a more favorable outcome in patients of diffuse midline glioma (61–63). In addition, baseline ADC values can be used as an outcome predictor in these tumors, although diffusion-derived metrics showed no significant association with overall survival (64).

Diffusion Tensor Imaging

Literature specifically dealing with diffusion-tensor imaging (DTI) in assessing “pediatric glioblastomas” is quite scarce. DTI is a more sophisticated quantitative analysis of diffusion-based imaging. In DTI, water movement is measured in several directions within the tissue from which tensors can be fit with directionality information. When these measurements are combined and analyzed, in addition to an averaged measure of water diffusion for each voxel (ADC), individual and summary measures of how water diffusion varies along different axes (fraction anisotropy—FA) can be calculated. Both ADC and FA reflect the microstructure of the tissue in which they are measured (65). For example, FA estimates the amount and the direction of diffusion restriction of water molecules along myelinated white matter tracts, which is in turn partly influenced by the degree of preserved and destroyed white matter tracts within the tumoral area (66–68).

DTI can demonstrate white matter tracts and their structural changes related to different brain pathologies. DTI describes the three-dimensional diffusion phenomenon of water molecules about their microenvironmental properties allowing a unique description of the space where this molecular movement occurs. This model provides an *in-vivo* demonstration of the complex ultrastructural organization of the white matter and structural changes due to tumor invasion. Current DTI and magnetic resonance tractography applications allow accurate graphic delineation of the eloquent white matter tracts and their relation with tumoral tissue, which may be essential in surgical treatment planning and useful in assessing post-therapeutic changes (69). Furthermore, DTI in mapping white matter tracts may sometimes enable resection of tumors previously deemed unresectable, such as well-defined pilocytic astrocytomas in the thalamus (Figure 9) (70).

Several authors demonstrated that the evaluation of the peritumoral area and the differentiation between tumoral infiltration and pure vasogenic edema might be enhanced by DTI analysis (68, 71–76). Other authors quantified tumoral and peritumoral FA in low- and high-grade gliomas with low-grade gliomas showing higher FA values than HGGs (76–80). The more conspicuous FA reduction in high-grade compared to low-grade

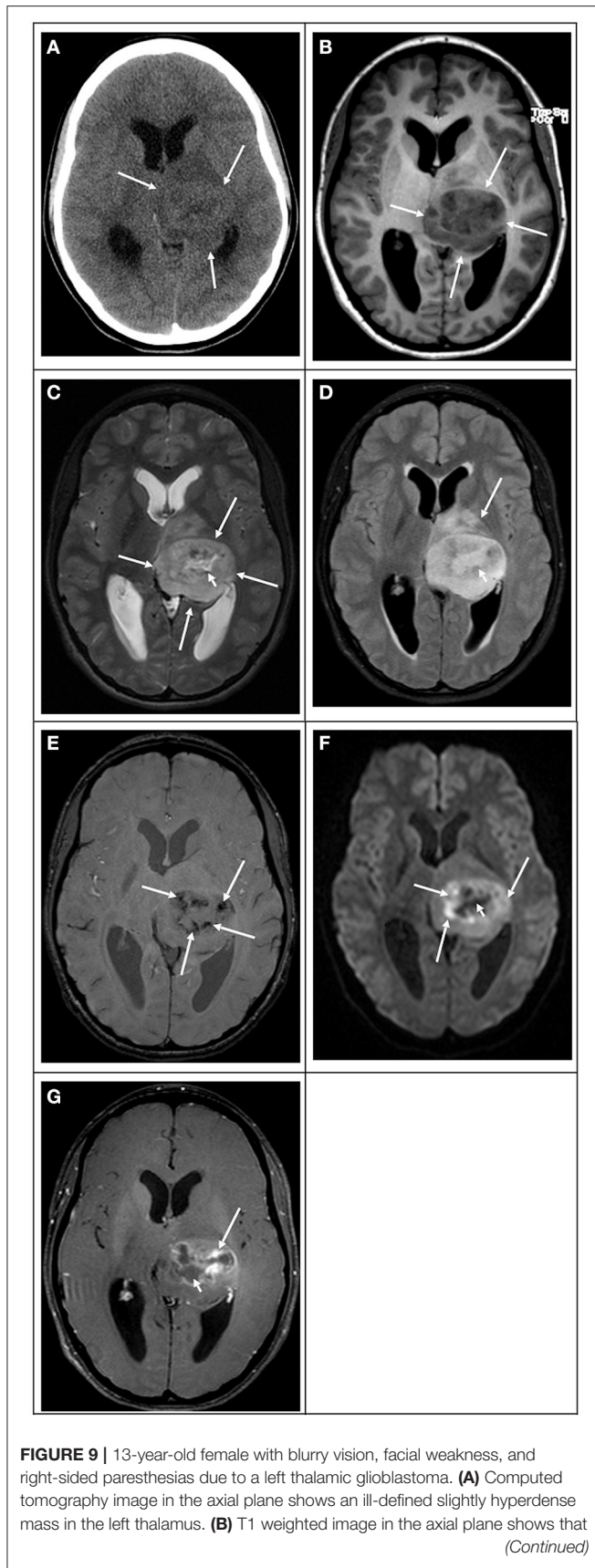


FIGURE 9 | 13-year-old female with blurry vision, facial weakness, and right-sided paresthesias due to a left thalamic glioblastoma. **(A)** Computed tomography image in the axial plane shows an ill-defined slightly hyperdense mass in the left thalamus. **(B)** T1 weighted image in the axial plane shows that
(Continued)

FIGURE 9 | the lesion is well-demarcated with heterogeneous mixed-signal, predominantly hypointense (white arrows). **(C)** T2 weighted image and **(D)** FLAIR images in the axial plane show that the bulk of the lesion is hyperintense (white arrows) with a central component showing even higher signal. **(E)** Susceptibility weighted image in the axial plane shows irregular signal drop foci within the tumoral bed (white arrows) in keeping with hemorrhage. **(F)** Diffusion-weighted image in the axial plane shows that the lesion is heterogeneous in signal. The periphery of the mass is isointense to the normal brain parenchyma. The center of the mass shows a hypointense signal (white arrow). Surrounding the center, there is an irregular hyperintense thick rim with low values in the ADC map (not shown) in keeping with restricted diffusion. **(G)** T1-weighted contrast-enhanced image in the axial plane shows that the tumor enhances heterogeneously. The thick irregular area that shows restricted diffusion enhances avidly (white arrows) with no enhancement centrally due to necrosis.

tumors is likely due to the higher incidence of cystic and necrotic changes leading to loss of white matter tract organization and integrity. Besides, some researchers also suggest that FA is more sensitive than ADC in the early detection of white matter tumoral involvement (67, 68, 78). White matter tract changes can occur due to fiber destruction (reduced absolute number), fiber edema (reduced density and higher water content), or fiber degradation (abnormal fibers with a normal number and density) (81, 82). In addition, qualitative assessment of DTI maps can suggest the different types of tumoral involvement such as displacement, edema, infiltration, destruction, or a combination of two or more, but one has to be careful of the technical limitations that may lead to false-negative tract visualization (68, 83–85).

Gauvain et al. (65) demonstrated the utility of ADC obtained via DTI assessing pediatric brain tumors. ADC correlated significantly with tumor cellularity and the calculated total nuclear area (nuclear area of each tumor cell type multiplied by the number of cells per high-power field). Brunberg et al. (51) found differences between ADC and FA from normal white matter and solid-enhancing tumor, cystic and necrotic areas, and regions of edema. However, they did not find differences in ADC values between various glioma subtypes.

DTI is also valuable in the assessment of postoperative changes. For example, DTI can compare the status of eloquent cortical pathways before and after the surgery delivering information to the neurosurgeon about the damaged and preserved tracts postoperatively (86–88). DTI also allows detecting and monitoring treatment-induced neurotoxicity in cerebral white matter (87, 89–92). Several studies investigating the effect of cranial irradiation and chemotherapy indicate a prominent decrease in mean FA values that are more severe in the frontal lobes compared with the parietal lobes despite the same radiation dose, suggesting regional susceptibility in the frontal lobe (89–94). Mabbott et al. (93) demonstrated that medulloblastomas treated with cranial-spinal radiation therapy show abnormal FA and ADC in the normal-appearing white matter. Their study observed damaged white matter microstructure and/or fiber integrity as demonstrated by FA and ADC for multiple regions within the cerebral hemispheres. Further, decreased FA and increased ADC were related to lower intellectual outcomes in patients relative to age-matched

controls. A significant advantage of DTI is that it provides measures sensitive to underlying tissue properties, and hence potential damage may be evident even within the normal-appearing white matter.

Perfusion Weighted Imaging

Perfusion weighted imaging (PWI) describes a group of valuable techniques that can non-invasively evaluate the cerebral hemodynamic status and, in many patients, can predict tumor grade and behavior (35, 51). The main clinically utilized PWI techniques include dynamic contrast-enhanced (DCE), dynamic susceptibility contrast (DSC), and arterial spin labeling (ASL). The main parameters derived from these techniques include cerebral blood volume (CBV), cerebral blood flow (CBF), and mean transit time (MTT), among others. Derivation of absolute perfusion parameters may be challenging at times, and therefore, relative CBV (rCBV) or relative CBF (rCBF) may be used when involved regions are normalized to other normal-appearing brain structures.

In general terms, most HGGs typically show higher perfusion (increased CBV and/or CBF) than low-grade gliomas (Figure 10). Nevertheless, compared to adults, the higher prevalence in children of malignant non-glioma neoplasms and contrast-enhancing low-grade tumors may confound the accuracy of grading of brain neoplasms using PWI measures in certain types of neoplasms.

Dynamic Susceptibility Contrast (DSC) Perfusion

DSC perfusion is the most widely used PWI technique and requires high-flow contrast injection, often using power injectors, and large-bore intravenous access, which may pose challenges in young children and infants (95). Other drawbacks of the DSC perfusion method are calcification and hemorrhage-induced susceptibility within the tumor and blood-brain barrier breakdown-related contrast leakage (96). Despite this, DSC is feasible and has been performed even in young children (97).

There is an overall significant difference in rCBV and CBF between pediatric low-grade gliomas and HGGs (98). In addition, in the study by Chang et al. (35), rCBV maps helped detect highly vascular areas correlated with areas of enhancement in three of their patients. rCBV maps may also demonstrate increased microvasculature even in the absence of enhancement in some patients with “glioblastoma” (35).

Dynamic Contrast Enhancement (DCE)

DCE may be used as a potential alternative or complementary technique to DSC. It has been mainly used in adult brain tumors, with few studies performed in children (99, 100). DCE provides signal intensity–time curve reflecting a combination of tissue perfusion, microvessel permeability, and extravascular-extracellular space characteristics (101, 102) thus allowing for a multiparametric characterization of tumor microvasculature and leakage quantitation.

The advantages of DCE over DSC are fewer susceptibility artifacts and the quantification of blood-brain barrier (BBB) integrity; indeed, the leading interest for DCE-derived metrics was initially focused on the volume transfer constant (Ktrans),

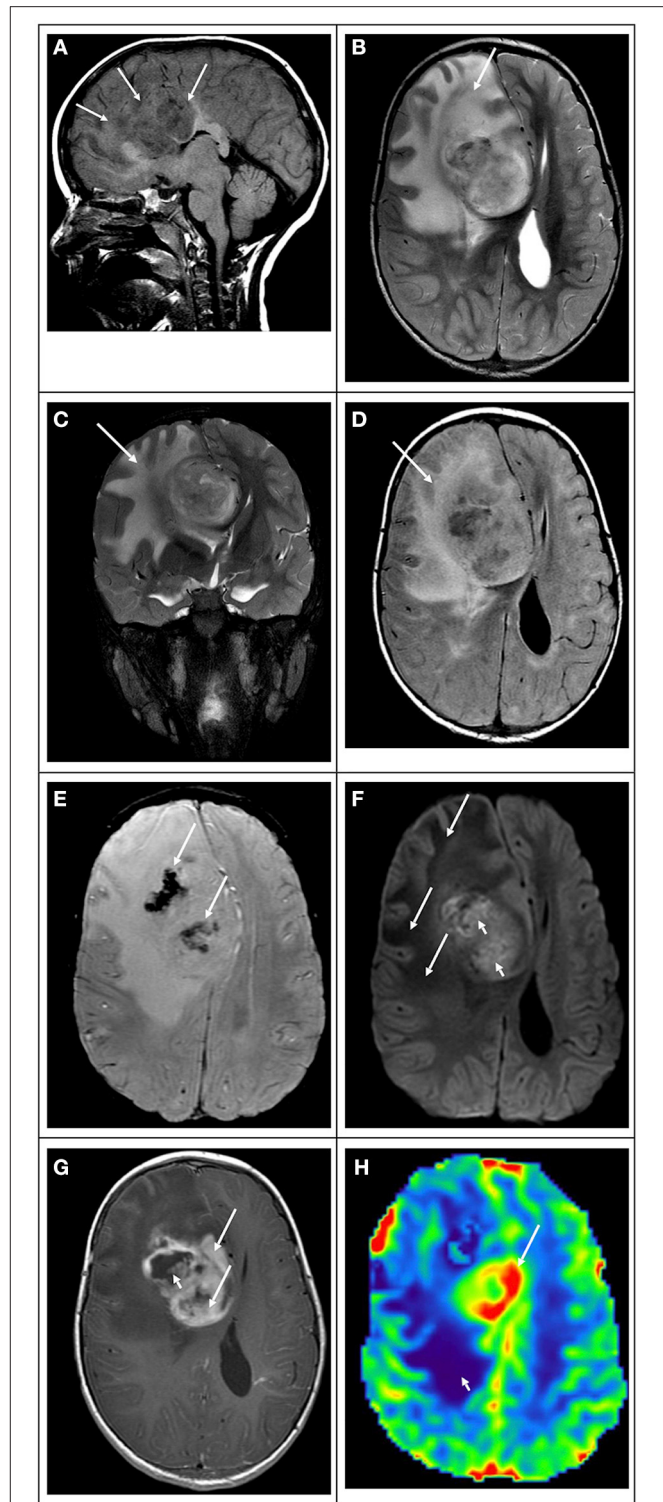


FIGURE 10 | 5-year-old male with headaches and confusion due to a right frontal “glioblastoma.” (A) T1 weighted image in the sagittal plane shows that the lesion is heterogeneous, ill-defined with mixed-signal, predominantly hypointense, and infiltrates the corpus callosum (white arrows). (B) T2 weighted image in the axial plane, (C) T2 weighted image in the coronal plane, and (D) FLAIR image in the axial plane show that the bulk of the lesion is
(Continued)

FIGURE 10 | hyperintense, with marked mass effect and vasogenic edema (white arrows). **(E)** Susceptibility weighted image in the axial plane shows irregular areas of signal drop within the tumoral bed (white arrows) in keeping with hemorrhage. **(F)** Diffusion-weighted image in the axial plane shows that the lesion is heterogeneous in signal. The extensive area of vasogenic edema shows low signals (white arrows). The midline component shows areas of hyperintense signal with low values in the ADC map (not shown) in keeping with restricted diffusion. **(G)** T1-weighted contrast-enhanced image in the axial plane shows that the tumor enhances heterogeneously. The midline component of the mass shows thick and irregular enhancement (white arrows) with no foci of enhancement in areas of necrosis (white arrowhead). **(H)** Arterial spin labeling perfusion image in the axial plane shows that the midline component has marked increased perfusion (white arrow). Note that the area of vasogenic edema is not associated with increased perfusion (white arrowhead).

a permeability marker correlating with BBB disruption (102) and malignancy (103). Conversely, DSC typically offers better temporal resolution than DCE, allowing potentially better blood volume estimation (104).

A small study demonstrated that DCE could be used to assess tumor grade in pediatric brain tumors, although not all were gliomas (100). Transfer constants from and into blood plasma (K_{trans} and K_{ep}) and extracellular extravascular volume fraction (V_e) showed a sensitivity of 71–76% and a specificity of 82–100% in separating low-grade from high-grade tumors. In another study, fractional plasma volume (V_p) was significantly different between high and low-grade tumors, but K_{trans} , K_{ep} , and V_e were not statistically different.

In a study of 64 pediatric brain tumor patients, Gupta et al. (105) demonstrated that DSC and DCE helped differentiate low-grade tumors, high-grade tumors, and amongst major posterior fossa tumors. rCBV and fractional plasma volume measures differed significantly between high-grade and low-grade tumors. High-grade tumors could be differentiated from low-grade tumors with an rCBV cutoff value of 2.41 and 88.6% sensitivity and 65% specificity. There was no significant difference in K_{trans} , K_{ep} , or V_e between these two groups of tumors (105).

Arterial Spin Labeling (ASL) Perfusion

ASL, a PWI technique that uses magnetically labeled water as endogenous contrast, has been used to study pediatric brain tumors (106). However, ASL is limited by a low signal-to-noise ratio, often the need for greater magnetic field strength, and the presence of susceptibility (105).

ASL is considered a reliable PWI technique in evaluating tumor perfusion and predicting glioma grade in adults (107). ASL is advantageous for children since it lacks contrast injection, the need for high flow injections, and has easier potential for CBF quantification. Also, ASL can be repeated if patients move (95). Moreover, younger children's immature paranasal sinuses also result in better ASL image quality, with potentially lesser degrees of distortion artifacts in the frontal and inferior brain regions (108).

In a study of ASL in pediatric brain tumors by Yeom et al. (95), the authors demonstrated that the technique could reasonably distinguish high-grade from low-grade tumors. Their

results in “glioblastoma” patients indicated that CBF in the tumoral bed might have a wide range, which suggests vascular heterogeneity similar to what is seen in patients with adult glioblastomas. According to these authors, ASL maps can depict tumor vascular heterogeneity and indicate higher tumor blood flow regions offering a valuable parameter to potentially direct biopsy of higher vascular density or more malignant regions (95). Dangouloff-Ros et al. (106) have confirmed that pediatric high-grade brain tumors generally display higher CBF than low-grade tumors on ASL. Low-grade gliomas had a significantly lower absolute CBF and rCBF than high-grade tumors (CBF: median, 29 mL/min/100g vs. median, 116 mL/min/100g; $P < 0.001$) (rCBF: median, 0.50 mL/min/100g vs. median, 2.21 mL/min/100g; $p < 0.001$). There was no significant difference between the various high-grade neoplasms (grade 3 gangliogliomas, glioblastomas, atypical teratoid rhabdoid tumor, and grade 3 ependymomas) (106). Morana et al. (109) compared ASL and DSC in 37 children with low-grade and HGGs obtained on a 1.5T scanner. Normalized CBV values in the most perfused area of each neoplasm were compared with normalized CBF from DSC and normalized CBF from ASL data and designated with a WHO tumor grade. According to the authors, normalized ASL provides comparable results to DSC and may help distinguish between low-grade and HGGs (109).

A meta-analysis of eight studies assessing pediatric glioma grading using ASL showed many bias and applicability issues. For low and high-grade tumor differentiation, the pooled sensitivity ranged from 0.69 to 0.92, and specificity ranged from 0.63 to 0.93 (110). Relative CBF demonstrated less variability than absolute CBF, as would be expected given the variability of acquisition techniques. In another meta-analysis, although not only composed of gliomas, normalized cerebral blood flow derived from ASL perfusion had 83% accuracy in separating low and high-grade pediatric brain tumors (111). Other authors have also confirmed that ASL can be a potentially valuable tool to differentiate low from high-grade tumors (106, 111–114) and that the technique has comparable results with DSC in the differentiation between low and HGGs (115).

Proton ^1H Magnetic Resonance Spectroscopy

Proton ^1H MRS is a non-invasive technique that has been used to evaluate tissue metabolism in a wide variety of diffuse and focal CNS diseases, including brain tumors (116). Several brain metabolites such as choline (Cho), N-acetylaspartate (NAA), creatine (Cr), myoinositol (mI), and lactate can show abnormalities in the context of brain neoplasms. For example, in gliomas, as tumor grade increases, there is an increase in the Cho/NAA ratio, reflecting increased metabolic activity. High Cho reflects rapid membrane turnover with glial proliferation, whereas low NAA reflects decreased normal neurons as they are replaced by neoplastic cells in the MRS voxel (35).

Multiple studies have demonstrated that a common feature of many rapidly growing tumors is a decreased NAA/Cr ratio and an increased lactate level (**Figure 11**) (37, 117–122). Cr concentration is supposedly rather stable over time,

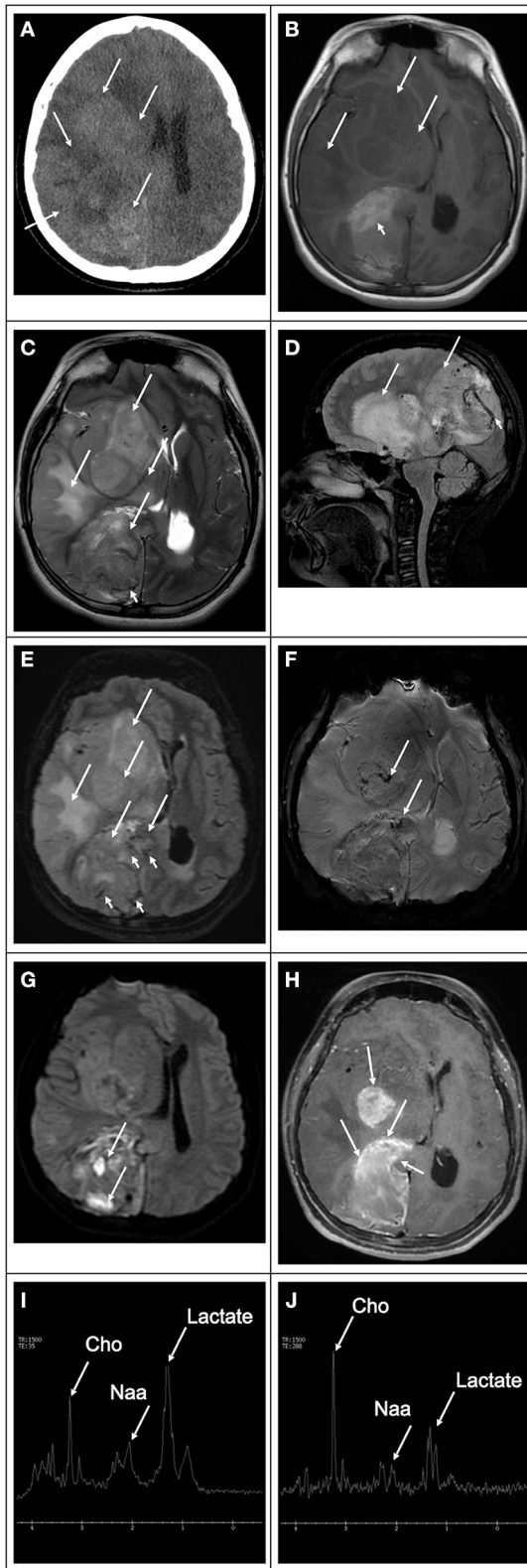


FIGURE 11 | 8-year-old- female with a hemispheric glioblastoma. **(A)** Computed tomography image in the axial plane shows an extensive mass in
(Continued)

FIGURE 11 | the right hemisphere (white arrows), causing mass effect, compression of the right lateral ventricle, and midline deviation. The lesion is heterogeneous with areas of hyper and hypodensity compatible with hemorrhage and edema, respectively. **(B)** T1 weighted image in the axial plane shows that the bulk of the lesion is hypointense (white arrows). There is a component of the mass that is high in signal intratumoral hemorrhage (white arrowhead). **(C)** T2 weighted image in the axial plane. **(D)** T2 weighted image in the sagittal plane, and **(E)** FLAIR image in the axial plane show that the lesion's bulk is hyperintense with marked mass effect vasogenic edema (white arrows). In addition, there is marked increased vascularity in the component located in the occipital region (white arrowheads). **(F)** Susceptibility weighted image in the axial plane shows scattered signal drop foci within the tumoral bed (white arrows) in keeping with hemorrhage. **(G)** Diffusion-weighted image in the axial plane shows that the lesion is heterogeneous in signal. The bulk of the lesion is isointense to the normal brain parenchyma with scattered hyperintense foci due to intratumoral hemorrhage (white arrows). **(H)** T1-weighted contrast-enhanced image in the axial plane shows that the tumor has multiple enhancing components heterogeneously. The mass has avid peripheral enhancement with internal non-enhancing elements in keeping with necrotic tissue. **(I,J)** Magnetic resonance spectroscopy obtained with short and long echo times showing marked decreased N-acetylaspartate peak, which corresponds to neuronal loss, increased choline peak, which corresponds to increase cell membrane turnover in an environment of rapid growing neoplastic tissue, and increased lactate peaks due to anaerobiosis and necrotic changes.

so it is used as a denominator to report the metabolite ratios in most studies. Elevated lipid-lactate peaks are more frequently found in HGGs, particularly in those undergoing central necrotic changes. Mixed MRI spectral patterns can reflect the known heterogeneity seen in many tumors (123). Importantly, patients with diffuse midline gliomas showing high levels of lactate on MRS are associated with poor prognosis (124).

Proton ^1H MRS may be used as an adjunct tool in the evaluation of “pediatric glioblastomas.” This technique has been applied for the initial diagnosis of brain masses, biopsy guidance, tumor grading, treatment response assessment, recurrence vs. treatment effects detection, and a prognostic marker in brain tumor patients. Higher Cho/Cr and Cho/NAA ratios are typically observed in HGGs compared to low-grade tumors and non-neoplastic masses in broad terms, although exceptions do occur (125). mI is often elevated in low-grade diffuse gliomas, unlike HGGs (123). Previous studies have shown that higher Cho/Cr and Cho/NAA ratios portray a poorer prognosis in pediatric brain tumors (126, 127). Other studies have looked at lactate/NAA ratios and normalized indices combining choline and lipid+lactate levels, demonstrating strong correlations with predictors of outcome (128, 129).

Pathogenic variants in the IDH1 and IDH2 can lead to the accumulation of abnormally high D-2-hydroxyglutarate (2-HG) levels in certain brain tumors. This increased 2-HG level may be detected *in-vivo* by specialized advanced spectral-edited MRS and used to characterize glial neoplasms. IDH1/2 pathogenic variants are considered prognostic biomarkers in subjects with glioma and are associated with more prolonged overall survival (24, 130). A meta-analysis demonstrated excellent sensitivity and specificity of 2-HG MRS to predict IDH mutant gliomas (131).

Chemical Exchange Saturation Transfer

Chemical exchange saturation transfer (CEST) is a recently developed technique that can identify very low concentrations of molecules by the presence of groups with exchangeable protons, such as hydroxyls, amides, and amines (132). The vast majority of studies on CEST and “glioblastomas” have been performed in adults. Future studies on “pediatric glioblastomas” are needed to confirm its utility in this age group. CEST signal is affected by endogenous proteins and metabolites such as glutamate, lactate, mI, and glucose that play crucial roles in tumor development, growth, and progression. Hence, studying these macromolecules and metabolites may help understand the brain tumor microenvironment and evaluate response to targeted therapies. Studies have demonstrated that CEST imaging can reasonably differentiate malignant neoplastic infiltration from peritumoral vasogenic edema, differentiate histopathological grades, and discriminate HGGs from the brain lymphomas (133). In addition, CEST can also reliably distinguish recurrent tumors from radiation necrosis (133). Moreover, the intensity of the CEST signal was shown to decrease in irradiated tumors at 3 days and 6 days post-treatment periods relative to baseline, suggesting that CEST may potentially help evaluate treatment response in brain tumors. CEST signal may potentially be an imaging biomarker for distinguishing true progression from pseudoprogression in “glioblastoma” patients (134).

Amide proton transfer (APT) imaging is a CEST technique that measures a decrease in bulk water intensity due to chemical exchange with magnetically labeled amide protons of endogenous proteins and peptides in tissues (135). Studies have shown the potential of APT-weighted imaging in delineating malignant neoplastic infiltration. In addition, the APT signal may also potentially be a valuable imaging biomarker for distinguishing true progression from pseudoprogression in glioblastoma patients (133). Studies have documented significantly higher APT signals in true progression cases than those with pseudoprogression (136). It is widely believed that active tumor cells express more protein species and higher concentrations of protein components, as shown by proteomics (136, 137) and proton MRS studies (138). In contrast to true progression, there are fewer mobile cytosolic proteins and peptides in regions of brain injury associated with pseudoprogression due to lower cellular density and disrupted cytoplasm. Collectively, these studies have indicated that APT based on CEST is fast emerging as a novel molecular MRI technique in neuro-oncology.

Multiparametric Analysis

Multiparametric analysis is an evolving method in which multiple quantitative MRI techniques are analyzed in combination to overcome the intrinsic limitations of conventional MRI and potentiate the individual value of each advanced MRI technique in isolation. For example, quantitative data obtained from metabolic and physiologic techniques such as DWI, DTI, DSC, DCE, ASL, or proton MRS can be variously combined and analyzed with multivariate logistic regression, analysis of variance, or artificial intelligence tools to determine the optimal parameter(s) and thresholds for addressing a specific question prediction.

Multiparametric MRI has been widely used to predict treatment response in glioblastoma patients, to differentiate glioblastoma from solitary brain metastasis (139), to differentiate radiation necrosis from a recurrent tumor (140), to assess tumor invasiveness (141), and to predict tumoral survival (142).

POSITRON EMISSION TOMOGRAPHY (PET)

Positron emission tomography (PET) is a nuclear medicine imaging modality that plays a vital role in evaluating brain tumors, including glioblastomas. PET, as a functional imaging technique, is typically used to complement anatomical imaging, capturing non-invasively functional and biochemical information about the tumor and its surroundings. This information is beneficial for tumor grading, differential diagnosis, tumor delineation, surgery planning, radiotherapy, and post-treatment monitoring follow-up (143). PET can probe the physiological milieu of neoplastic cells, such as glucose metabolism, protein synthesis, and DNA replication. There are multiple groups of PET radionuclide tracers typically used to evaluate tumor metabolism, including glucose metabolism tracers, amino acid tracers, and other miscellaneous tracers that can target various receptors or functions of the cells. These PET tracers are useful in demonstrating cellular proliferation, hypoxia sensing, and inflammation (144).

A typical and widely used glucose metabolism tracer is 18F-2-fluoro-2-deoxy-D-glucose ([18F]FDG). [18F]FDG is taken up by the glucose transporter, engaging in phosphorylation (the first step of glucose metabolism), and subsequently becomes trapped in the cell (145). [18F]FDG demonstrates avid uptake in the brain, which may limit the interpretation of tumors near or involving the gray matter (144). On the other hand, amino acid transport tracers exhibit lower uptake in normal tissue, being more sensitive than 18F-FDG in primary and recurrent tumors, and are helpful in differentiating recurrent tumors from treatment-induced changes (146). Typical amino acid analogs include [11C]11C-methyl-methionine ([11C]MET), 3,4-dihydroxy-6-[18F]-fluoro-L-phenylalanine ([18F]FDOPA), O-(2-[18F]-fluoroethyl)-L-tyrosine ([18F]FET), and deoxynucleoside bases such as [18F]fluoro-thymidine and [18F]clofarabine (143, 145).

[11C]MET is the most studied and validated amino acid tracer. It is an essential amino acid for protein synthesis and is considered more sensitive than [18F]FDG in delineation of tumors. [11C]MET is avidly taken up by glioma cells, with only a low uptake in normal cerebral tissue. Several studies have suggested that tumor uptake of [11C]MET mainly reflects increased amino acid transport (147). Its most important limitation is its very short life (144). 18F-labeled amino acids have been created to increase amino acid tracer half-life and utilization, namely [18F]FET and [18F]FDOPA. [18F]FET is a tracer for both HGGs as well as low-grade gliomas due to an efficient nucleophilic reaction, elevated uptake by tumor tissues, low uptake by inflammatory tissues, and high stability (148). [18F]FDOPA is incorporated into cells through amino

acid transporters that are overexpressed in gliomas, and its transport and uptake are independent of the blood-brain barrier (149). [18F]FDOPA has shown a significant correlation between WHO grade and the volume of MRI contrast enhancement and volume of T2 hyperintensity (150). Another radiotracer, [18F]fluorothymidine ([18F]FLT), is a thymidine analog uptaken in tissues after phosphorylation by the thymidine kinase (151). Thymidine kinase is considered a critical enzyme in the DNA salvage pathway. Nucleotide salvage pathways recover bases and nucleosides that are formed during the degradation of RNA and DNA (152). Since [18F]FLT has lower uptake in the normal brain, it correlates well with proliferative tissue markers (153). The radiotracer has been used in diagnosis and assessment of glioma grading, in differentiating tumor recurrence from radionecrosis, in assessing response to treatment, and in predicting overall survival (154).

PET tracers such as the [18F]Fluoromisonidazole, which sense oxygen levels in cells, can be used to visualize hypoxia. Hypoxia is an essential feature of most solid tumors (153, 155). For example, in a hypoxic tumor microenvironment, radiation therapy could be more effective at a higher dose (143). Inflammation, a component of the immune response, is well-known to occur in glioblastomas. Translocator protein (TSPO) is a component of the mitochondrial membrane protein responsible for cholesterol transport and responds to cell stress. Broadly, TSPO is treated as a biomarker sensitive to pro-inflammatory stimuli (143). Moreover, TSPO PET imaging was found to be correlated with outcome (156).

As neuro-oncology treatment advances and therapies centered on tumor biomarkers are discovered, the development of selective PET tracers can dramatically enhance the efforts toward personalized medicine (143).

TREATMENT

The standard of care for adult glioblastomas involves surgery with maximal safe tumor resection followed by chemoradiation as adjuvant treatment (157). There is not such a well-defined standard of care for “pediatric glioblastomas.” Regarding surgery, substantial evidence recommends the adoption of maximal safe surgical resection of the visible tumor, since prognosis correlates positively with the amount of tumor resected (5, 6, 16, 158, 159). However, the choice of adjuvant treatment is debated due to the potentially deleterious effects of radiation treatment in the early developing brain and inconsistent results of various chemotherapy regimens (9). Radiation therapy has become the standard of treatment, particularly for those children older than 3 years with a newly diagnosed “glioblastoma” (36). Younger children, however, are more susceptible to the adverse effects associated with radiation therapy and are typically treated with chemotherapy alone and radiation-sparing approaches (160–162).

Novel classes of treatments such as molecular-targeted therapy and immunotherapy have been recently incorporated as new weapons in the arsenal of treatment of oncology patients (163). Immunotherapy agents include typically chimeric

antigen receptor (CAR) T-cell therapy, immune checkpoint inhibitors, virotherapy, cancer vaccines, and dendritic cell therapy. Molecular-targeted therapy consists of drugs or other substances that target specific molecules involved in the growth and spread of cancer cells (164). The most common targets for molecular-targeted therapy in pediatric brain tumors, in particular, HGGs and other high-grade tumors, are the tyrosine kinase (165), tumor-specific surface proteins (monoclonal antibodies) (166), vascular endothelial growth factor (167), platelet-derived growth factor and epidermal growth factor, PI3K-mTOR pathway (mostly animal model studies) (168), ERK-RAS-RAF mitogen-activated protein kinase pathway (BRAF mutation) (169), e PI3K/AKT pathway, gene fusions (170), Sonic Hedgehog pathway (171), and epigenetic targets (DNA methylation, chromatin modeling, and histone modifications signaling) (172). Despite multiple clinical trials in pediatric brain tumors, molecular-targeted therapy, with some exceptions, has not yet made a major impact on survival or, for that matter, quality-of-life for children with brain tumors (164). However, there remains great promise for the future as more agents are developed and included in clinical trials.

CARs are synthetic receptors composed of three major components (an extracellular tumor-specific antibody, an intracellular signaling structure, and a transmembrane domain serving as a bridge), which are typically added to a T cell, augmenting its function (173–175). These receptors allow T cells to recognize and destroy specific cancer cells without the major histocompatibility complex (MHC) presentation (176). In normal conditions, T cells require costimulation by the antigen-presenting cell to exert their cytolytic activity (177). This method has had tremendous success in treating leukemias. CAR T cell administration can be made hematogenously, or via the cerebral spinal fluid, or locally in the tumor cavity. Brain tumors are currently one of the most common solid tumor types undergoing clinical trial testing for CAR T cell efficacy and have shown early promise in treating “glioblastomas” (178, 179). Multiple clinical trials are evaluating the efficacy of CAR T cell therapy in solid tumors. However, none are FDA approved yet.

Checkpoint inhibitors are a group of drugs that target signaling pathways involved in the modulation of host immune responses as part of the normal regulation of immunity and establishment of tolerance. However, neoplastic cells are known to block these checkpoints and suppress the host’s immune response, bypassing immune recognition and destruction (180). Exhaustion is a phenomenon that occurs during cancer progression, which refers to immune cell desensitization. At exhaustion, T cells are unable to kill malignant cells (181, 182), which can occur when neoplastic cells upregulate inhibitory receptors such as programmed cell death receptor-1 ligand (PD-L1) and cytotoxic T lymphocyte antigen-4 (CTLA-4) (183). Checkpoint inhibitors seek to reverse this inhibition so that an immune response can be mounted against the malignant cells (180). Researchers have shown that 75–100% of gliomas in a sample of patients exhibited PD-L1 expression, which correlated with the severity of the disease (184, 185).

There are several studies describing the efficacy and side effect profile of checkpoint inhibitors in pediatric patients.

A clinical trial conducted by Gorski et al. (186) in recurrent or refractory pediatric brain tumors treated with the immune checkpoint inhibitor nivolumab demonstrated transient partial responses in patients with positive PD-L1 expression and higher tumor mutation burden. Nivolumab was well-tolerated with some transient partial responses in patients with positive PD-L1 expression and a higher tumor mutation burden. Median survival for PD-L1 positive patients was 13.7 weeks vs. 4.2 weeks for PD-L1 negative patients ($p = 0.08$). These findings suggest that only tumors with elevated PD-L1 expression and tumor mutation burden may benefit from immune checkpoint inhibitors (186). A clinical trial by Cacciotti et al. (187) involving PD-1 and CTLA-4 blockade has shown relatively well tolerability in a group of pediatric patients with DIPG, HGG, ependymoma, craniopharyngioma, high-grade neuroepithelial tumor, and non-germinomatous germ cell tumor. The majority of the patients, during the time of the study, showed stable disease or partial response. Checkpoint inhibition has proved to be a promising new form of immunotherapy, demonstrating efficacy in adult malignancies such as melanoma, renal cell carcinoma, and small cell lung cancer; however, it has failed to produce durable responses in pediatric brain cancer (188).

Virotherapy is an emerging technique that uses viruses as therapeutic agents. Oncolytic viruses combine tumor cell destruction and immune system stimulation, which are the most critical components of virotherapy (189). In addition, viruses can also be used as vectors for gene therapy, inducing the expression of a transgene that modifies the immune environment to promote an anti-tumor response (189). Several oncolytic viruses have been evaluated clinically in pediatric brain tumors, such as myxoma virus (190, 191), recombinant poliovirus (192, 193), adenovirus (194), Seneca Valley-001 (195), reovirus (196), herpesvirus (197), and Newcastle disease virus (198). The administration of oncolytic viruses can be either intravenous or intratumoral. Once the virus reaches the tumor, it can infect both normal and neoplastic cells; however, it only replicates and destroys the tumor cells (198). Cancer vaccines are typically well-tolerated and contain tumor antigens, such as peptides, tumor lysate, nucleic acids, and autologous dendritic cells (196, 199). Mutations such as the H3 K27M in DIPG have been explored as a target for peptide vaccines (199). A number of clinical trials are evaluating the efficacy of virotherapy in pediatric brain tumors. However, none are FDA approved yet.

Dendritic cells are an essential link between the innate and adaptive immune systems. Upon finding foreign antigens, dendritic cells release inflammatory cytokines that activate the immune system. These cells also process and present antigens to T cells and B cells, thereby activating naïve, effector, and memory immune cells or maintaining tolerance against self-antigens (200). For active immunotherapy, dendritic cells are typically generated by isolating monocytes from cancer patients that are expanded and activated *ex vivo*. These cells are loaded with either tumor lysate, peptides, nucleic acids, or viral epitopes that are expressed by the tumor. Dendritic cells are usually matured with GM-CSF, a critical cytokine, then administered as a vaccine. Adjuvants such as tetanus toxoid are important to improve inflammation and immunogenicity in the host (200). Dendritic

cell vaccines have demonstrated modest but encouraging results in patients with advanced cancers (201). It is thought that these vaccines can induce tumor-specific T cell responses and immunological memory, constituting a promising platform for pediatric brain tumors (201). There are several trials using dendritic cell vaccines and tumor RNA (201) or tumor lysate for pediatric brain tumors (202, 203). Dendritic cell vaccines are reliably manufactured and extremely well-tolerated; however, for efficacy improvement, enhanced techniques for targeting, antigen loading, and migration *in vivo* are needed (196). There are a number of dendritic cell vaccines in clinical trials; none are available for widespread clinical use.

Immunotherapy has shown efficacy against lymphoid tumors and some solid neoplasms, with less efficacy in the treatment of pediatric brain tumors. Reasons for this limited response include tumor heterogeneity, a suppressive immune microenvironment, and the blood-brain barrier (163). In addition, most pediatric brain tumors are immunologically quiescent, with a low mutational burden. Therefore, immunotherapy strategies should be tailored based on the type of tumor being targeted and its associated microenvironment (163). According to the National Cancer Institute at the National Institutes of Health, there are only six FDA-approved immunotherapy options for brain and nervous system tumors, namely dostarlimab, a checkpoint inhibitor that targets the PD-1/PD-L1 pathway for patients with advanced cases associated with DNA mismatch repair deficiency; granulocyte-macrophage colony-stimulating factor, an immunomodulatory cytokine combined with naxitamab-gqgk, for advanced cases of neuroblastoma; pembrolizumab, a checkpoint inhibitor that targets the PD-1/PD-L1 pathway for patients with advanced cases associated with high microsatellite instability, DNA mismatch repair deficiency, or high tumor mutational burden; bevacizumab, a monoclonal antibody that targets the VEGF/VEGFR pathway and inhibits tumor blood vessel growth for advanced “glioblastoma”; dinutuximab, a monoclonal antibody that targets the GD2 pathway for first-line treatment of high-risk pediatric neuroblastoma; naxitamab-gqgk, a monoclonal antibody that targets the GD2 pathway and approved in combination with GM-CSF for a subset of patients with advanced neuroblastoma.

Regardless of the treatment selected, “pediatric glioblastoma” remains a devastating disease, with median survival ranging from 13 to 73 months, with a 5 year survival of <20% (4–6, 204). Nevertheless, several studies have demonstrated a relatively better prognosis and long-term survival among pediatric patients compared to adults (5–7).

FINAL REMARKS

Glioblastomas are highly aggressive neoplasms that represent a small subset of pediatric brain tumors. “Pediatric glioblastomas” are grossly and microscopically identical to their adult counterparts, but molecularly and genetically distinct. These differences may explain why “pediatric glioblastomas” may have a different prognosis or occasionally be less responsive to current adjuvant therapy regimens.

MRI is the imaging modality of choice in evaluating “pediatric glioblastomas,” not only because it is safer due to the absence of radiation exposure but also for its superior spatial and contrast resolution and for delivering physiologic information about the tumor and adjacent brain parenchyma. MRI is also vital for surgical and radiation therapy planning and postsurgical evaluation. Conventional MRI sequences provide precise anatomic detail and detection of blood-brain barrier integrity and leakage. Advanced MRI techniques such as DWI, PWI, and proton ^1H MRS may help differentiate non-enhancing tumors from other causes of changes in the signal. It is expected that continued research increases the availability of advanced MRI techniques. This increment, coupled with emerging MRI

techniques and advances in personalized medical care, perhaps powered by artificial intelligence techniques, would hopefully result in a better quality of life and overall improvement in survival rates.

AUTHOR CONTRIBUTIONS

All authors listed have made a substantial, direct and intellectual contribution to the work, and approved it for publication.

ACKNOWLEDGMENTS

The authors thank Lydia Sheldon for proofreading and edits.

REFERENCES

- Louis DN, Perry A, Wesseling P, Brat DJ, Cree IA, Figarella-Branger D, et al. The 2021 WHO classification of tumors of the central nervous system: a summary. *Neuro Oncol.* (2021) 23:1231–51. doi: 10.1093/neuonc/noab106
- Adamson C, Kanu OO, Mehta AI, Di C, Lin N, Mattox AK, et al. Glioblastoma multiforme: a review of where we have been and where we are going. *Expert Opin Investig Drugs.* (2009) 18:1061–83. doi: 10.1517/13543780903052764
- Artico M, Cervoni L, Celli P, Salvati M, Palma L. Supratentorial glioblastoma in children: a series of 27 surgically treated cases. *Childs Nerv Syst.* (1993) 9:7–9. doi: 10.1007/BF00301926
- Perkins SM, Rubin JB, Leonard JR, Smyth MD, El Naqa I, Michalski JM, et al. Glioblastoma in children: a single-institution experience. *Int J Radiat Oncol Biol Phys.* (2011) 80:1117–21. doi: 10.1016/j.ijrobp.2010.03.013
- Das KK, Mehrotra A, Nair AP, Kumar S, Srivastava AK, Sahu RN, et al. Pediatric glioblastoma: clinico-radiological profile and factors affecting the outcome. *Childs Nerv Syst.* (2012) 28:2055–62. doi: 10.1007/s00381-012-1890-x
- Nikitović M, Stanić D, Pekmezović T, Gazibara MS, Bokun J, Paripović L, et al. Pediatric glioblastoma: a single institution experience. *Childs Nerv Syst.* (2016) 32:97–103. doi: 10.1007/s00381-015-2945-6
- Broniscer A, Gajjar A. Supratentorial high-grade astrocytoma and diffuse brainstem glioma: two challenges for the pediatric oncologist. *Oncologist.* (2004) 9:197–206. doi: 10.1634/theoncologist.9-2-197
- Wolff B, Ng A, Roth D, Parthey K, Warmuth-Metz M, Eyrych M, et al. Pediatric high grade glioma of the spinal cord: results of the HIT-GBM database. *J Neurooncol.* (2012) 107:139–46. doi: 10.1007/s11060-011-0718-y
- Das KK, Kumar R. Pediatric glioblastoma. In: De Vleeschouwer S, editor. *Glioblastoma*. Brisbane, AU: Codon Publications (2017).
- Epstein F, Wisoff J. Intra-axial tumors of the cervicomedullary junction. *J Neurosurg.* (1987) 67:483–7. doi: 10.3171/jns.1987.67.4.0483
- Milano GM, Cerri C, Ferruzzi V, Capolsini I, Mastrodicasa E, Genitori L, et al. Congenital glioblastoma. *Pediatr Blood Cancer.* (2009) 53:124–6. doi: 10.1002/pbc.22008
- Fangusaro J. Pediatric high-grade gliomas and diffuse intrinsic pontine gliomas. *J Child Neurol.* (2009) 24:1409–17. doi: 10.1177/0883073809338960
- Chaichana K, Parker S, Olivi A, Quiñones-Hinojosa A. A proposed classification system that projects outcomes based on preoperative variables for adult patients with glioblastoma multiforme. *J Neurosurg.* (2010) 112:997–1004. doi: 10.3171/2009.9.JNS09805
- Moini J, Piran P, editors. *Histophysiology*. In: *Functional and Clinical Neuroanatomy*. London: Elsevier (2020). p. 1–49.
- Suri V, Das P, Pathak P, Jain A, Sharma MC, Borkar SA, et al. Pediatric glioblastomas: a histopathological and molecular genetic study. *Neuro Oncol.* (2009) 11:274–80. doi: 10.1215/15228517-2008-092
- Mahvash M, Hugo H-H, Maslehaty H, Mehdorn HM, Stark AM. Glioblastoma multiforme in children: report of 13 cases and review of the literature. *Pediatr Neurol.* (2011) 45:178–80. doi: 10.1016/j.pediatrneurol.2011.05.004
- Urbańska K, Sokołowska J, Szmidi M, Sysa P. Glioblastoma multiforme - an overview. *Contemp Oncol.* (2014) 18:307–12. doi: 10.5114/wo.2014.40559
- Paulino AC, Mai WY, Chintagumpala M, Taher A, Teh BS. Radiation-induced malignant gliomas: is there a role for reirradiation? *Int J Radiat Oncol Biol Phys.* (2008) 71:1381–7. doi: 10.1016/j.ijrobp.2007.12.018
- Louis DN, Perry A, Reifenberger G, von Deimling A, Figarella-Branger D, Cavenee WK, et al. The 2016 World Health Organization classification of tumors of the central nervous system: a summary. *Acta Neuropathol.* (2016) 131:803–20. doi: 10.1007/s00401-016-1545-1
- Reinhardt A, Stichel D, Schrimpf D, Koelsche C, Wefers AK, Ebrahimi A, et al. Tumors diagnosed as cerebellar glioblastoma comprise distinct molecular entities. *Acta Neuropathol Commun.* (2019) 7:163. doi: 10.1186/s40478-019-0801-8
- International Agency for Research on Cancer, Wiestler OD. *WHO Classification of Tumours of the Central Nervous System*. International Agency for Research on Cancer (2016).
- Pollack IF, Hamilton RL, Sobol RW, Nikiforova MN, Lyons-Weiler MA, LaFramboise WA, et al. IDH1 mutations are common in malignant gliomas arising in adolescents: a report from the Children’s Oncology Group. *Childs Nerv Syst.* (2011) 27:87–94. doi: 10.1007/s00381-010-1264-1
- Pollack IF, Finkelstein SD, Woods J, Burnham J, Holmes EJ, Hamilton RL, et al. Expression of p53 and prognosis in children with malignant gliomas. *N Engl J Med.* (2002) 346:420–7. doi: 10.1056/NEJMoa012224
- Mackay A, Burford A, Carvalho D, Izquierdo E, Fazal-Salom J, Taylor KR, et al. Integrated molecular meta-analysis of 1,000 pediatric high-grade and diffuse intrinsic pontine glioma. *Cancer Cell.* (2017) 32:520–37.e5. doi: 10.1016/j.ccell.2017.08.017
- Sturm D, Witt H, Hovestadt V, Khuong-Quang DA, Jones DT, Konermann C, et al. Hotspot mutations in H3F3A and IDH1 define distinct epigenetic and biological subgroups of glioblastoma. *Cancer Cell.* (2012) 224:425–37. doi: 10.1016/j.ccr.2012.08.024
- Pratt D, Natarajan SK, Banda A, Giannini C, Vats P, Koschmann C, et al. Circumscribed/non-diffuse histology confers a better prognosis in H3K27M-mutant gliomas. *Acta Neuropathol.* (2018) 135:299–301. doi: 10.1007/s00401-018-1805-3
- Castel D, Philippe C, Calmon R, Le Dret L, Truffaux N, Boddaert N, et al. Histone H3F3A and HIST1H3B K27M mutations define two subgroups of diffuse intrinsic pontine gliomas with different prognosis and phenotypes. *Acta Neuropathol.* (2015) 130:815–27. doi: 10.1007/s00401-015-1478-0
- Brat DJ, Aldape K, Colman H, Holland EC, Louis DN, Jenkins RB, et al. cIMPACT-NOW update 3: recommended diagnostic criteria for “Diffuse astrocytic glioma, IDH-wildtype, with molecular features of glioblastoma, WHO grade IV”. *Acta Neuropathol.* (2018) 136:805–10. doi: 10.1007/s00401-018-1913-0
- Paugh BS, Zhu X, Qu C, Endersby R, Diaz AK, Zhang J, et al. Novel oncogenic PDGFRA mutations in pediatric high-grade gliomas. *Cancer Res.* (2013) 73:6219–29. doi: 10.1158/0008-5472.CAN-13-1491
- Hegi ME, Diserens A-C, Gorlia T, Hamou M-F, de Tribolet N, Weller M, et al. MGMT gene silencing and benefit from temozolomide in glioblastoma. *N Engl J Med.* (2005) 352:997–1003. doi: 10.1056/NEJMoa043331

31. Lee JY, Park C-K, Park S-H, Wang K-C, Cho B-K, Kim S-K. MGMT promoter gene methylation in pediatric glioblastoma: analysis using MS-MLPA. *Childs Nerv Syst.* (2011) 27:1877–83. doi: 10.1007/s00381-011-1525-7
32. Donson AM, Addo-Yobo SO, Handler MH, Gore L, Foreman NK. MGMT promoter methylation correlates with survival benefit and sensitivity to temozolomide in pediatric glioblastoma. *Pediatr Blood Cancer.* (2007) 48:403–7. doi: 10.1002/pbc.20803
33. Korshunov A, Ryzhova M, Hovestadt V, Bender S, Sturm D, Capper D, et al. Integrated analysis of pediatric glioblastoma reveals a subset of biologically favorable tumors with associated molecular prognostic markers. *Acta Neuropathol.* (2015) 129:669–78. doi: 10.1007/s00401-015-1405-4
34. Banan R, Christians A, Bartels S, Lehmann U, Hartmann C. Absence of MGMT promoter methylation in diffuse midline glioma, H3 K27M-mutant. *Acta Neuropathol Commun.* (2017) 5:98. doi: 10.1186/s40478-017-0500-2
35. Chang Y-W, Yoon H-K, Shin H-J, Roh HG, Cho JM. MR imaging of glioblastoma in children: usefulness of diffusion/perfusion-weighted MRI and MR spectroscopy. *Pediatr Radiol.* (2003) 33:836–42. doi: 10.1007/s00247-003-0968-8
36. Fangusaro J. Pediatric high grade glioma: a review and update on tumor clinical characteristics and biology. *Front Oncol.* (2012) 2:105. doi: 10.3389/fonc.2012.00105
37. Panigrahy A, Blüml S. Neuroimaging of pediatric brain tumors: from basic to advanced magnetic resonance imaging (MRI). *J Child Neurol.* (2009) 24:1343–65. doi: 10.1177/0883073809342129
38. Knopp EA, Cha S, Johnson G, Mazumdar A, Golfinos JG, Zagzag D, et al. Glial neoplasms: dynamic contrast-enhanced T2*-weighted MR imaging. *Radiology.* (1999) 211:791–8. doi: 10.1148/radiology.211.3.r99j n46791
39. Shin JH, Lee HK, Kwun BD, Kim J-S, Kang W, Choi CG, et al. Using relative cerebral blood flow and volume to evaluate the histopathologic grade of cerebral gliomas: preliminary results. *AJR Am J Roentgenol.* (2002) 179:783–9. doi: 10.2214/ajr.179.3.1790783
40. Tien RD, Felsberg GJ, Friedman H, Brown M, MacFall J. MR imaging of high-grade cerebral gliomas: value of diffusion-weighted echoplanar pulse sequences. *AJR Am J Roentgenol.* (1994) 162:671–7. doi: 10.2214/ajr.162.3.8109520
41. Le Bihan D, Lima M, Federau C, Sigmund EE. *Intravoxel Incoherent Motion (IVIM) MRI: Principles and Applications.* Singapore: CRC Press (2018).
42. Svolos P, Kousi E, Kapsalaki E, Theodorou K, Fezoulidis I, Kappas C, et al. The role of diffusion and perfusion weighted imaging in the differential diagnosis of cerebral tumors: a review and future perspectives. *Cancer Imaging.* (2014) 14:20. doi: 10.1186/1470-7330-14-20
43. Le Bihan D, Turner R, Douek P, Patronas N. Diffusion MR imaging: clinical applications. *AJR Am J Roentgenol.* (1992) 159:591–9. doi: 10.2214/ajr.159.3.1503032
44. Eis M, Els T, Hoehn-Berlage M, Hossmann KA. Quantitative diffusion MR imaging of cerebral tumor and edema. *Acta Neurochir Suppl.* (1994) 60:344–6. doi: 10.1007/978-3-7091-9334-1_92
45. Krabbe K, Gideon P, Wagn P, Hansen U, Thomsen C, Madsen F. MR diffusion imaging of human intracranial tumours. *Neuroradiology.* (1997) 39:483–9. doi: 10.1007/s002340050450
46. Ebisu T, Tanaka C, Umeda M, Kitamura M, Naruse S, Higuchi T, et al. Discrimination of brain abscess from necrotic or cystic tumors by diffusion-weighted echo planar imaging. *Magn Reson Imaging.* (1996) 14:1113–6. doi: 10.1016/S0730-725X(96)00237-8
47. Okamoto K, Ito J, Ishikawa K, Sakai K, Tokiguchi S. Diffusion-weighted echo-planar MR imaging in differential diagnosis of brain tumors and tumor-like conditions. *Eur Radiol.* (2000) 10:1342–50. doi: 10.1007/s0033099000310
48. Dutt SN, Mirza S, Chavda SV, Irving RM. Radiologic differentiation of intracranial epidermoids from arachnoid cysts. *Otol Neurotol.* (2002) 23:84–92. doi: 10.1097/00129492-200201000-00019
49. Camacho DLA, Smith JK, Castillo M. Differentiation of toxoplasmosis and lymphoma in AIDS patients by using apparent diffusion coefficients. *AJNR Am J Neuroradiol.* (2003) 24:633–7.
50. Messina C, Bignone R, Bruno A, Bruno A, Bruno F, Calandri M, et al. Diffusion-weighted imaging in oncology: an update. *Cancers.* (2020) 12:1493. doi: 10.3390/cancers12061493
51. Brunberg JA, Chenevert TL, McKeever PE, Ross DA, Junck LR, Muraszko KM, et al. *In vivo* MR determination of water diffusion coefficients and diffusion anisotropy: correlation with structural alteration in gliomas of the cerebral hemispheres. *AJNR Am J Neuroradiol.* (1995) 16:361–71.
52. Nadal Desbarats L, Herlidou S, de Marco G, Gondry-Jouet C, Le Gars D, Deramond H, et al. Differential MRI diagnosis between brain abscesses and necrotic or cystic brain tumors using the apparent diffusion coefficient and normalized diffusion-weighted images. *Magn Reson Imaging.* (2003) 21:645–50. doi: 10.1016/S0730-725X(03)00084-5
53. Muccio CF, Caranci F, D'Arco F, Cerase A, De Lipsis L, Esposito G, et al. Magnetic resonance features of pyogenic brain abscesses and differential diagnosis using morphological and functional imaging studies: a pictorial essay. *J Neuroradiol.* (2014) 41:153–67. doi: 10.1016/j.neurad.2014.05.004
54. Higano S, Yun X, Kumabe T, Watanabe M, Mugikura S, Umetsu A, et al. Malignant astrocytic tumors: clinical importance of apparent diffusion coefficient in prediction of grade and prognosis. *Radiology.* (2006) 241:839–46. doi: 10.1148/radiol.2413051276
55. Kan P, Liu JK, Hedlund G, Brockmeyer DL, Walker ML, Kestle JRW. The role of diffusion-weighted magnetic resonance imaging in pediatric brain tumors. *Childs Nerv Syst.* (2006) 22:1435–9. doi: 10.1007/s00381-006-0229-x
56. Wang Q-P, Lei D-Q, Yuan Y, Xiong N-X. Accuracy of ADC derived from DWI for differentiating high-grade from low-grade gliomas: systematic review and meta-analysis. *Medicine.* (2020) 99:e19254. doi: 10.1097/MD.00000000000019254
57. Asao C, Korogi Y, Hotta A, Shimomura O, Kitajima M, Negi A, et al. Orbital pseudotumors: value of short inversion time inversion-recovery MR imaging. *Radiology.* (1997) 202:55–9. doi: 10.1148/radiology.202.1.8988192
58. Hein PA, Eskey CJ, Dunn JE, Hug EB. Diffusion-weighted imaging in the follow-up of treated high-grade gliomas: tumor recurrence versus radiation injury. *AJNR Am J Neuroradiol.* (2004) 25:201–9.
59. Chenevert TL, Stegman LD, Taylor JM, Robertson PL, Greenberg HS, Rehemtulla A, et al. Diffusion magnetic resonance imaging: an early surrogate marker of therapeutic efficacy in brain tumors. *J Natl Cancer Inst.* (2000) 92:2029–36. doi: 10.1093/jnci/92.24.2029
60. Evelhoch JL. Magnetic resonance measurement of tumor perfusion and vascularity. In: Shields AF, Price P, editors. *In Vivo Imaging of Cancer Therapy.* Cancer Drug Discovery and Development. Totowa, NJ: Humana Press. doi: 10.1007/978-1-59745-341-7_5
61. Poussaint TY, Kocak M, Vajapeyam S, Packer RI, Robertson RL, Geyer R, et al. MRI as a central component of clinical trials analysis in brainstem glioma: a report from the Pediatric Brain Tumor Consortium (PBTC). *Neuro Oncol.* (2011) 13:417–27. doi: 10.1093/neuonc/naq200
62. Lober RM, Cho Y-J, Tang Y, Barnes PD, Edwards MS, Vogel H, et al. Diffusion-weighted MRI derived apparent diffusion coefficient identifies prognostically distinct subgroups of pediatric diffuse intrinsic pontine glioma. *J Neurooncol.* (2014) 117:175–82. doi: 10.1007/s11060-014-1375-8
63. Aboian MS, Tong E, Solomon DA, Kline C, Gautam A, Vardapetyan A, et al. Diffusion characteristics of pediatric diffuse midline gliomas with histone H3-K27M mutation using apparent diffusion coefficient histogram analysis. *AJNR Am J Neuroradiol.* (2019) 40:1804–10. doi: 10.3174/ajnr.A6302
64. Ceschin R, Kocak M, Vajapeyam S, Pollack IF, Onar-Thomas A, Dunkel IJ, et al. Quantifying radiation therapy response using apparent diffusion coefficient (ADC) parametric mapping of pediatric diffuse intrinsic pontine glioma: a report from the pediatric brain tumor consortium. *J Neurooncol.* (2019) 143:79–86. doi: 10.1007/s11060-019-03133-y
65. Gauvain KM, McKinstry RC, Mukherjee P, Perry A, Neil JJ, Kaufman BA, et al. Evaluating pediatric brain tumor cellularity with diffusion-tensor imaging. *AJR Am J Roentgenol.* (2001) 177:449–54. doi: 10.2214/ajr.177.2.1770449
66. Basser PJ. Inferring microstructural features and the physiological state of tissues from diffusion-weighted images. *NMR Biomed.* (1995) 8:333–44. doi: 10.1002/nbm.1940080707
67. Lori NE, Akbudak E, Shimony JS, Cull TS, Snyder AZ, Guillery RK, et al. Diffusion tensor fiber tracking of human brain connectivity: acquisition methods, reliability analysis and biological results. *NMR Biomed.* (2002) 15:494–515. doi: 10.1002/nbm.779
68. Field AS, Alexander AL, Wu Y-C, Hasan KM, Witwer B, Badie B. Diffusion tensor eigenvector directional color imaging patterns in the evaluation of

- cerebral white matter tracts altered by tumor. *J Magn Reson Imaging*. (2004) 20:555–62. doi: 10.1002/jmri.20169
69. Bulakbaşı N. Diffusion-tensor imaging in brain tumors. *Imaging Med*. (2009) 1:155–71. doi: 10.2217/iim.09.20
 70. Moshel YA, Elliott RE, Monoky DJ, Wisoff JH. Role of diffusion tensor imaging in resection of thalamic juvenile pilocytic astrocytoma. *J Neurosurg Pediatr*. (2009) 4:495–505. doi: 10.3171/2009.7.PEDS09128
 71. Lu S, Ahn D, Johnson G, Law M, Zagzag D, Grossman RI. Diffusion-tensor MR imaging of intracranial neoplasia and associated peritumoral edema: introduction of the tumor infiltration index. *Radiology*. (2004) 232:221–8. doi: 10.1148/radiol.2321030653
 72. Provenzale JM, McGraw P, Mhatre P, Guo AC, Delong D. Peritumoral brain regions in gliomas and meningiomas: investigation with isotropic diffusion-weighted MR imaging and diffusion-tensor MR imaging. *Radiology*. (2004) 232:451–60. doi: 10.1148/radiol.2322030959
 73. Morita K-I, Matsuzawa H, Fujii Y, Tanaka R, Kwee IL, Nakada T. Diffusion tensor analysis of peritumoral edema using lambda chart analysis indicative of the heterogeneity of the microstructure within edema. *J Neurosurg*. (2005) 102:336–41. doi: 10.3171/jns.2005.102.2.0336
 74. Tsuchiya K, Fujikawa A, Nakajima M, Honya K. Differentiation between solitary brain metastasis and high-grade glioma by diffusion tensor imaging. *Br J Radiol*. (2005) 78:533–7. doi: 10.1259/bjr/68749637
 75. Price SJ, Jena R, Burnet NG, Hutchinson PJ, Dean AF, Peña A, et al. Improved delineation of glioma margins and regions of infiltration with the use of diffusion tensor imaging: an image-guided biopsy study. *AJNR Am J Neuroradiol*. (2006) 27:1969–74.
 76. Stadlbauer A, Ganslandt O, Buslei R, Hammen T, Gruber S, Moser E, et al. Gliomas: histopathologic evaluation of changes in directionality and magnitude of water diffusion at diffusion-tensor MR imaging. *Radiology*. (2006) 240:803–10. doi: 10.1148/radiol.2403050937
 77. Tropine A, Vucurevic G, Delani P, Boor S, Hopf N, Bohl J, et al. Contribution of diffusion tensor imaging to delineation of gliomas and glioblastomas. *J Magn Reson Imaging*. (2004) 20:905–12. doi: 10.1002/jmri.20217
 78. Goebell E, Paustenbach S, Vaeterlein O, Ding X-Q, Heese O, Fiehler J, et al. Low-grade and anaplastic gliomas: differences in architecture evaluated with diffusion-tensor MR imaging. *Radiology*. (2006) 239:217–22. doi: 10.1148/radiol.2383050059
 79. Nilsson D, Rutka JT, Snead OC III, Raybaud CR, Widjaja E. Preserved structural integrity of white matter adjacent to low-grade tumors. *Childs Nerv Syst*. (2008) 24:313–20. doi: 10.1007/s00381-007-0466-7
 80. Yuan W, Holland SK, Jones BV, Crone K, Mangano FT. Characterization of abnormal diffusion properties of supratentorial brain tumors: a preliminary diffusion tensor imaging study. *J Neurosurg Pediatr*. (2008) 1:263–9. doi: 10.3171/PED/2008/1/4/263
 81. Field AS. Diffusion tensor imaging at the crossroads: fiber tracking meets tissue characterization in brain tumors. *AJNR Am J Neuroradiol*. (2005) 26:2168–9.
 82. Roberts TPL, Liu F, Kassner A, Mori S, Guha A. Fiber density index correlates with reduced fractional anisotropy in white matter of patients with glioblastoma. *AJNR Am J Neuroradiol*. (2005) 26:2183–6.
 83. Jellison BJ, Field AS, Medow J, Lazar M, Salamat MS, Alexander AL. Diffusion tensor imaging of cerebral white matter: a pictorial review of physics, fiber tract anatomy, and tumor imaging patterns. *AJNR Am J Neuroradiol*. (2004) 25:356–69.
 84. Helton KJ, Phillips NS, Khan RB, Boop FA, Sanford RA, Zou P, et al. Diffusion tensor imaging of tract involvement in children with pontine tumors. *AJNR Am J Neuroradiol*. (2006) 27:786–93.
 85. Yen PS, Teo BT, Chiu CH, Chen SC, Chiu TL, Su CF. White Matter tract involvement in brain tumors: a diffusion tensor imaging analysis. *Surg Neurol*. (2009) 72:464–9; discussion 469. doi: 10.1016/j.surneu.2009.05.008
 86. Laundre BJ, Jellison BJ, Badie B, Alexander AL, Field AS. Diffusion tensor imaging of the corticospinal tract before and after mass resection as correlated with clinical motor findings: preliminary data. *AJNR Am J Neuroradiol*. (2005) 26:791–6.
 87. Yu CS, Li KC, Xuan Y, Ji XM, Qin W. Diffusion tensor tractography in patients with cerebral tumors: a helpful technique for neurosurgical planning and postoperative assessment. *Eur J Radiol*. (2005) 56:197–204. doi: 10.1016/j.ejrad.2005.04.010
 88. Lui YW, Law M, Chacko-Mathew J, Babb JS, Tuvia K, Allen JC, et al. Brainstem corticospinal tract diffusion tensor imaging in patients with primary posterior fossa neoplasms stratified by tumor type. *Neurosurgery*. (2007) 61:1199–208. doi: 10.1227/01.neu.0000306098.38141.81
 89. Khong PL, Kwong DL, Chan GC, Sham JS, Chan FL, Ooi GC. Diffusion-tensor imaging for the detection and quantification of treatment-induced white matter injury in children with medulloblastoma: a pilot study. *AJNR Am J Neuroradiol*. (2003) 24:734–40.
 90. Leung LHT, Ooi GC, Kwong DLW, Chan GCF, Cao G, Khong PL. White-matter diffusion anisotropy after chemo-irradiation: a statistical parametric mapping study and histogram analysis. *Neuroimage*. (2004) 21:261–8. doi: 10.1016/j.neuroimage.2003.09.020
 91. Qiu D, Leung LHT, Kwong DLW, Chan GCF, Khong P-L. Mapping radiation dose distribution on the fractional anisotropy map: applications in the assessment of treatment-induced white matter injury. *Neuroimage*. (2006) 31:109–15. doi: 10.1016/j.neuroimage.2005.12.007
 92. Qiu D, Kwong DLW, Chan GCF, Leung LHT, Khong P-L. Diffusion tensor magnetic resonance imaging finding of discrepant fractional anisotropy between the frontal and parietal lobes after whole-brain irradiation in childhood medulloblastoma survivors: reflection of regional white matter radiosensitivity? *Int. J Radiat Oncol Biol Phys*. (2007) 69:846–51. doi: 10.1016/j.ijrobp.2007.04.041
 93. Mabbott DJ, Noseworthy MD, Bouffet E, Rockel C, Laughlin S. Diffusion tensor imaging of white matter after cranial radiation in children for medulloblastoma: correlation with IQ. *Neuro Oncol*. (2006) 8:244–52. doi: 10.1215/15228517-2006-002
 94. Welzel T, Niethammer A, Mende U, Heiland S, Wenz F, Debus J, et al. Diffusion tensor imaging screening of radiation-induced changes in the white matter after prophylactic cranial irradiation of patients with small cell lung cancer: first results of a prospective study. *AJNR Am J Neuroradiol*. (2008) 29:379–83. doi: 10.3174/ajnr.A0797
 95. Yeom KW, Mitchell LA, Lober RM, Barnes PD, Vogel H, Fisher PG, et al. Arterial Spin-Labelled Perfusion of Pediatric Brain Tumors. *AJNR Am J Neuroradiol*. (2014) 35:395–401. doi: 10.3174/ajnr.A3670
 96. Lacerda S, Law M. Magnetic resonance perfusion and permeability imaging in brain tumors. *Neuroimaging Clin N Am*. (2009) 19:527–57. doi: 10.1016/j.nic.2009.08.007
 97. Gaudino S, Martucci M, Botto A, Ruberto E, Leone E, Infante A, et al. Brain DSC MR perfusion in children: a clinical feasibility study using different technical standards of contrast administration. *AJNR Am J Neuroradiol*. (2019) 40:359–65. doi: 10.3174/ajnr.A5954
 98. Dallery F, Bouzerar R, Michel D, Attencourt C, Promelle V, Peltier J, et al. Perfusion magnetic resonance imaging in pediatric brain tumors. *Neuroradiology*. (2017) 59:1143–53. doi: 10.1007/s00234-017-1917-9
 99. Miyazaki K, Jerome NP, Collins DJ, Orton MR, d'Arcy JA, Wallace T, et al. Demonstration of the reproducibility of free-breathing diffusion-weighted MRI and dynamic contrast enhanced MRI in children with solid tumors: a pilot study. *Eur Radiol*. (2015) 25:2641–50. doi: 10.1007/s00330-015-3666-7
 100. Vajapeyam S, Stamoulis C, Ricci K, Kieran M, Poussaint TY. Automated processing of dynamic contrast-enhanced MRI: correlation of advanced pharmacokinetic metrics with tumor grade in pediatric brain tumors. *AJNR Am J Neuroradiol*. (2017) 38:170–5. doi: 10.3174/ajnr.A4949
 101. Essig M, Nguyen TB, Shiroishi MS, Saake M, Provenzale JM, Enterline DS, et al. Perfusion MRI: the five most frequently asked clinical questions. *AJR Am J Roentgenol*. (2013) 201:W495–510. doi: 10.2214/AJR.12.9543
 102. Heye AK, Culling RD, Valdés Hernández MDC, Thrippleton MJ, Wardlaw JM. Assessment of blood-brain barrier disruption using dynamic contrast-enhanced MRI. A systematic review. *Neuroimage Clin*. (2014) 6:262–74. doi: 10.1016/j.nicl.2014.09.002
 103. Li X, Zhu Y, Kang H, Zhang Y, Liang H, Wang S, et al. Glioma grading by microvascular permeability parameters derived from dynamic contrast-enhanced MRI and intratumoral susceptibility signal on susceptibility weighted imaging. *Cancer Imaging*. (2015) 15:4. doi: 10.1186/s40644-015-0039-z
 104. Anzalone N, Castellano A, Cadioli M, Conte GM, Cuccarini V, Bizzi A, et al. Brain gliomas: multicenter standardized assessment of dynamic contrast-enhanced and dynamic susceptibility contrast MR images. *Radiology*. (2018) 287:933–43. doi: 10.1148/radiol.2017170362

105. Gupta PK, Saini J, Sahoo P, Patir R, Ahlawat S, Beniwal M, et al. Role of dynamic contrast-enhanced perfusion magnetic resonance imaging in grading of pediatric brain tumors on 3T. *Pediatr Neurosurg.* (2017) 52:298–305. doi: 10.1159/000479283
106. Dangouloff-Ros V, Deroulers C, Foissac F, Badoual M, Shotar E, Grévent D, et al. Arterial spin labeling to predict brain tumor grading in children: correlations between histopathologic vascular density and perfusion MR imaging. *Radiology.* (2016) 281:553–66. doi: 10.1148/radiol.2016152228
107. Warmuth C, Gunther M, Zimmer C. Quantification of blood flow in brain tumors: comparison of arterial spin labeling and dynamic susceptibility-weighted contrast-enhanced MR imaging. *Radiology.* (2003) 228:523–32. doi: 10.1148/radiol.2282020409
108. Deibler AR, Pollock JM, Kraft RA, Tan H, Burdette JH, Maldjian JA. Arterial spin-labeling in routine clinical practice, part 1: technique and artifacts. *AJNR Am J Neuroradiol.* (2008) 29:1228–34. doi: 10.3174/ajnr.A1030
109. Morana G, Tortora D, Staglianò S, Nozza P, Mascelli S, Severino M, et al. Pediatric astrocytic tumor grading: comparison between arterial spin labeling and dynamic susceptibility contrast MRI perfusion. *Neuroradiology.* (2018) 60:437–46. doi: 10.1007/s00234-018-1992-6
110. Delgado AF, De Luca F, van Westen D, Delgado AF. Arterial spin labeling MR imaging for differentiation between high- and low-grade glioma—a meta-analysis. *Neuro Oncol.* (2018) 20:1450–61. doi: 10.1093/neuonc/ny095
111. Hales PW, d'Arco F, Cooper J, Pfeuffer J, Hargrave D, Mankad K, et al. Arterial spin labelling and diffusion-weighted imaging in paediatric brain tumours. *Neuroimage Clin.* (2019) 22:101696. doi: 10.1016/j.nicl.2019.101696
112. Hales PW, Phipps KP, Kaur R, Clark CA. A two-stage model for *in vivo* assessment of brain tumor perfusion and abnormal vascular structure using arterial spin labeling. *PLoS ONE.* (2013) 8:e75717. doi: 10.1371/journal.pone.0075717
113. Dangouloff-Ros V, Grevent D, Pagès M, Blauwblomme T, Calmon R, Elie C, et al. Choroid plexus neoplasms: toward a distinction between carcinoma and papilloma using arterial spin-labeling. *AJNR Am J Neuroradiol.* (2015) 36:1786–90. doi: 10.3174/ajnr.A4332
114. Kikuchi K, Hiwatashi A, Togao O, Yamashita K, Yoshimoto K, Mizoguchi M, et al. Correlation between arterial spin-labeling perfusion and histopathological vascular density of pediatric intracranial tumors. *J Neurooncol.* (2017) 135:561–9. doi: 10.1007/s11060-017-2604-8
115. ElBeheiry AA, Emara DM, Abdel-Latif AA-B, Abbas M, Ismail AS. Arterial spin labeling in the grading of brain gliomas: could it help? *Egyptian J Radiol Nucl Med.* (2020) 51:1–11. doi: 10.1186/s43055-020-00352-6
116. Brandão LA, Poussaint TY. Pediatric brain tumors. *Neuroimaging Clin N Am.* (2013) 233:499–525. doi: 10.1016/j.nic.2013.03.003
117. Sutton LN, Wang Z, Gusnard D, Lange B, Perilongo G, Bogdan AR, et al. Proton magnetic resonance spectroscopy of pediatric brain tumors. *Neurosurgery.* (1992) 31:195–202. doi: 10.1227/00006123-199208000-00004
118. Ott D, Hennig J, Ernst T. Human brain tumors: assessment with *in vivo* proton MR spectroscopy. *Radiology.* (1993) 186:745–52. doi: 10.1148/radiology.186.3.8430183
119. Shimizu H, Kumabe T, Tominaga T, Kayama T, Hara K, Ono Y, et al. Noninvasive evaluation of malignancy of brain tumors with proton MR spectroscopy. *AJNR Am J Neuroradiol.* (1996) 17:737–47.
120. Tien RD, Lai PH, Smith JS, Lazeyras F. Single-voxel proton brain spectroscopy exam (PROBE/SV) in patients with primary brain tumors. *AJR Am J Roentgenol.* (1996) 167:201–9. doi: 10.2214/ajr.167.1.8659372
121. Meyerand ME, Pipas JM, Mamourian A, Tosteson TD, Dunn JF. Classification of biopsy-confirmed brain tumors using single-voxel MR spectroscopy. *AJNR Am J Neuroradiol.* (1999) 20:117–23.
122. Lemort M, Canizares-Perez AC, Van der Stappen A, Kampouridis S. Progress in magnetic resonance imaging of brain tumours. *Curr Opin Oncol.* (2007) 19:616–22. doi: 10.1097/CCO.0b013e3282f076b2
123. Zarifi M, Tzika AA. Proton MRS imaging in pediatric brain tumors. *Pediatr Radiol.* (2016) 46:952–62. doi: 10.1007/s00247-016-3547-5
124. Yamasaki E, Kurisu K, Kajiwara Y, Watanabe Y, Takayasu T, Akiyama Y, et al. Magnetic resonance spectroscopic detection of lactate is predictive of a poor prognosis in patients with diffuse intrinsic pontine glioma. *Neuro Oncol.* (2011) 13:791–801. doi: 10.1093/neuonc/nor038
125. Chawla S, Lee S-C, Mohan S, Wang S, Nasrallah M, Vossough A, et al. Lack of choline elevation on proton magnetic resonance spectroscopy in grade I-III gliomas. *Neuroradiol J.* (2019) 32:250–8. doi: 10.1177/1971400919846509
126. Girard N, Wang ZJ, Erbetta A, Sutton LN, Phillips PC, Rorke LB, et al. Prognostic value of proton MR spectroscopy of cerebral hemisphere tumors in children. *Neuroradiology.* (1998) 40:121–5. doi: 10.1007/s002340050551
127. Warren KE, Frank JA, Black JL, Hill RS, Duyn JH, Aikin AA, et al. Proton magnetic resonance spectroscopic imaging in children with recurrent primary brain tumors. *J Clin Oncol.* (2000) 18:1020. doi: 10.1200/JCO.2000.18.5.1020
128. Tarnawski R, Sokol M, Pieniazek P, Maciejewski B, Walecki J, Miszczyk L, et al. 1H-MRS *in vivo* predicts the early treatment outcome of postoperative radiotherapy for malignant gliomas. *Int J Radiat Oncol Biol Phys.* (2002) 52:1271–6. doi: 10.1016/S0360-3016(01)02769-9
129. Marcus K, Astrakas L, Zurakowski D, Zarifi M, Mintzopoulos D, Poussaint T, et al. Predicting survival of children with CNS tumors using proton magnetic resonance spectroscopic imaging biomarkers. *Int J Oncol.* (2007) 30:651–7. doi: 10.3892/ijo.30.3.651
130. Sanson M, Marie Y, Paris S, Idbaih A, Laffaire J, Ducray F, et al. Isocitrate dehydrogenase 1 codon 132 mutation is an important prognostic biomarker in gliomas. *J Clin Oncol.* (2009) 27:4150–4. doi: 10.1200/JCO.2009.21.9832
131. Suh CH, Kim HS, Jung SC, Choi CG, Kim SJ. 2-Hydroxyglutarate MR spectroscopy for prediction of isocitrate dehydrogenase mutant glioma: a systemic review and meta-analysis using individual patient data. *Neuro Oncol.* (2018) 20:1573–83. doi: 10.1093/neuonc/ny113
132. Jones KM, Pollard AC, Pagel MD. Clinical applications of chemical exchange saturation transfer (CEST) MRI. *J Magn Reson Imaging.* (2018) 47:11–27. doi: 10.1002/jmri.25838
133. Zhou J, Heo H-Y, Knutsson L, van Zijl PCM, Jiang S. APT-weighted MRI: Techniques, current neuro applications, and challenging issues. *J Magn Reson Imaging.* (2019) 50:347–64. doi: 10.1002/jmri.26645
134. Regnery S, Adeberg S, Dreher C, Oberhollenzer J, Meissner J-E, Goerke S, et al. Chemical exchange saturation transfer MRI serves as predictor of early progression in glioblastoma patients. *Oncotarget.* (2018) 9:28772–83. doi: 10.18632/oncotarget.25594
135. Zhou J, Payen J-F, Wilson DA, Traystman RJ, van Zijl PCM. Using the amide proton signals of intracellular proteins and peptides to detect pH effects in MRI. *Nat Med.* (2003) 9:1085–90. doi: 10.1038/nm907
136. Ma B, Blakeley JO, Hong X, Zhang H, Jiang S, Blair L, et al. Applying amide proton transfer-weighted MRI to distinguish pseudoprogression from true progression in malignant gliomas. *J Magn Reson Imaging.* (2016) 44:456–62. doi: 10.1002/jmri.25159
137. Hobbs SK, Shi G, Homer R, Harsh G, Scott W, Atlas, et al. Magnetic resonance image-guided proteomics of human glioblastoma multiforme. *J Magn Reson Imaging.* (2003) 18:530–6. doi: 10.1002/jmri.10395
138. Isobe T, Matsumura A, Anno I, Yoshizawa T, Nagatomo Y, Itai Y, et al. Quantification of cerebral metabolites in glioma patients with proton MR spectroscopy using T2 relaxation time correction. *Magn Reson Imaging.* (2002) 20:343–9. doi: 10.1016/S0730-725X(02)00500-3
139. Chen XZ, Yin XM, Ai L, Chen Q, Li SW, Dai JP. Differentiation between brain glioblastoma multiforme and solitary metastasis: qualitative and quantitative analysis based on routine MR imaging. *AJNR Am J Neuroradiol.* (2012) 33:1907–12. doi: 10.3174/ajnr.A3106
140. Nael K, Bauer AH, Hormigo A, Lemole M, Germano IM, Puig J, et al. Multiparametric MRI for differentiation of radiation necrosis from recurrent tumor in patients with treated glioblastoma. *AJR Am J Roentgenol.* (2018) 210:18–23. doi: 10.2214/AJR.17.18003
141. Li C, Wang S, Yan J-L, Torheim T, Boonzaier NR, Sinha R, et al. Characterizing tumor invasiveness of glioblastoma using multiparametric magnetic resonance imaging. *J Neurosurg.* (2019) 132:1465–72. doi: 10.3171/2018.12.JNS182926
142. Stringfield O, Arrington JA, Johnston SK, Rognin NG, Peeri NC, Balagurunathan Y, et al. Multiparameter MRI predictors of long-term survival in glioblastoma multiforme. *Tomography.* (2019) 5:135–44. doi: 10.18383/j.tom.2018.00052
143. Drake LR, Hillmer AT, Cai Z. Approaches to PET imaging of glioblastoma. *Molecules.* (2020) 25:568. doi: 10.3390/molecules25030568

144. Verger A, Langen KJ. PET imaging in glioblastoma: use in clinical practice. In: *Glioblastoma*. Codon Publications (2017). Available online at: <https://www.ncbi.nlm.nih.gov/books/NBK469986/>
145. Som P, Atkins HL, Bandoypadhyay D, Fowler JS, MacGregor RR, Matsui K, et al. A fluorinated glucose analog, 2-fluoro-2-deoxy-D-glucose (F-18): nontoxic tracer for rapid tumor detection. *J Nucl Med*. (1980) 21:670–5.
146. von Neubeck C, Seidlitz A, Kitzler HH, Beuthien-Baumann B, Krause M. Glioblastoma multiforme: emerging treatments and stratification markers beyond new drugs. *Br J Radiol*. (2015) 88:20150354. doi: 10.1259/bjr.20150354
147. Grosu A-L, Weber WA, Riedel E, Jeremic B, Nieder C, Franz M, et al. L-(methyl-11C) methionine positron emission tomography for target delineation in resected high-grade gliomas before radiotherapy. *Int J Radiat Oncol Biol Phys*. (2005) 63:64–74. doi: 10.1016/j.ijrobp.2005.01.045
148. Wang L, Lieberman BP, Ploessl K, Kung HF. Synthesis and evaluation of ¹⁸F labeled FET prodrugs for tumor imaging. *Nucl Med Biol*. (2014) 41:58–67. doi: 10.1016/j.nucmedbio.2013.09.011
149. Janvier L, Olivier P, Blonski M, Morel O, Vignaud J-M, Karcher G, et al. Correlation of SUV-derived indices with tumoral aggressiveness of gliomas in static 18F-FDOPA pet: use in clinical practice. *Clin Nucl Med*. (2015) 40:e429–35. doi: 10.1097/RLU.0000000000000897
150. Patel CB, Fazzari E, Chakhoyan A, Yao J, Raymond C, Nguyen H, et al. F-FDOPA PET and MRI characteristics correlate with degree of malignancy and predict survival in treatment-naïve gliomas: a cross-sectional study. *J Neurooncol*. (2018) 139:399–409. doi: 10.1007/s11060-018-2877-6
151. Toyohara J, Waki A, Takamatsu S, Yonekura Y, Magata Y, Fujibayashi Y. Basis of FLT as a cell proliferation marker: comparative uptake studies with [³H]thymidine and [³H]arabinothymidine, and cell-analysis in 22 asynchronously growing tumor cell lines. *Nucl Med Biol*. (2002) 29:281–7. doi: 10.1016/S0969-8051(02)00286-X
152. Been LB, Suurmeijer AJH, Cobben DCP, Jager PL, Hoekstra HJ, Elsinga PH. [¹⁸F]FLT-PET in oncology: current status and opportunities. *Eur J Nucl Med Mol Imaging*. (2004) 31:1659–72. doi: 10.1007/s00259-004-1687-6
153. Yamamoto Y, Ono Y, Aga F, Kawai N, Kudomi N, Nishiyama Y. Correlation of 18F-FLT uptake with tumor grade and Ki-67 immunohistochemistry in patients with newly diagnosed and recurrent gliomas. *J Nucl Med*. (2012) 53:1911–5. doi: 10.2967/jnumed.112.104729
154. Zhao F, Cui Y, Li M, Fu Z, Chen Z, Kong L, et al. Prognostic value of 3'-deoxy-3'-18F-fluorothymidine ([¹⁸F] FLT PET) in patients with recurrent malignant gliomas. *Nucl Med Biol*. (2014) 41:710–5. doi: 10.1016/j.nucmedbio.2014.04.134
155. Horsman MR, Mortensen LS, Petersen JB, Busk M, Overgaard J. Imaging hypoxia to improve radiotherapy outcome. *Nat Rev Clin Oncol*. (2012) 9:674–87. doi: 10.1038/nrclinonc.2012.171
156. Vlodaysky E, Soustiel JF. Immunohistochemical expression of peripheral benzodiazepine receptors in human astrocytomas and its correlation with grade of malignancy, proliferation, apoptosis and survival. *J Neurooncol*. (2007) 81:1–7. doi: 10.1007/s11060-006-9199-9
157. Stupp R, Mason WP, van den Bent MJ, Weller M, Fisher B, Taphoorn MJB, et al. Radiotherapy plus concomitant and adjuvant temozolomide for glioblastoma. *N Engl J Med*. (2005) 352:987–96. doi: 10.1056/NEJMoa043330
158. Packer RJ. Diagnosis and treatment of pediatric brain tumors. *Curr Opin Neurol*. (1994) 7:484–91. doi: 10.1097/00019052-199412000-00003
159. Finlay JL, Boyett JM, Yates AJ, Wisoff JH, Milstein JM, Geyer JR, et al. Randomized phase III trial in childhood high-grade astrocytoma comparing vincristine, lomustine, and prednisone with the eight-drugs-in-1-day regimen. *Childrens Cancer Group J Clin Oncol*. (1995) 13:112–23. doi: 10.1200/JCO.1995.13.1.112
160. Geyer JR, Finlay JL, Boyett JM, Wisoff J, Yates A, Mao L, et al. Survival of infants with malignant astrocytomas. A Report from the Childrens Cancer Group. *Cancer*. (1995) 75:1045–50.
161. Dufour C, Grill J, Lellouch-Tubiana A, Puget S, Chastagner P, Frappaz D, et al. High-grade glioma in children under 5 years of age: a chemotherapy only approach with the BBSFOP protocol. *Eur J Cancer*. (2006) 42:2939–45. doi: 10.1016/j.ejca.2006.06.021
162. Sanders RP, Kocak M, Burger PC, Merchant TE, Gajjar A, Broniscer A. High-grade astrocytoma in very young children. *Pediatr Blood Cancer*. (2007) 49:888–93. doi: 10.1002/pbc.21272
163. Foster JB, Madsen PJ, Hegde M, Ahmed N, Cole KA, Maris JM, et al. Immunotherapy for pediatric brain tumors: past and present. *Neuro Oncol*. (2019) 21:1226–38. doi: 10.1093/neuonc/noz077
164. Packer RJ, Kilburn L. Molecular-targeted therapy for childhood brain tumors: a moving target. *J Child Neurol*. (2020) 35:791–8. doi: 10.1177/0883073820931635
165. Wetmore C, Daryani VM, Billups CA, Boyett JM, Leary S, Tanos R, et al. Phase II evaluation of sunitinib in the treatment of recurrent or refractory high-grade glioma or ependymoma in children: a children's Oncology Group Study ACNS1021. *Cancer Med*. (2016) 5:1416–24. doi: 10.1002/cam4.713
166. Chatwin HV, Cruz Cruz J, Green AL. Pediatric high-grade glioma: moving toward subtype-specific multimodal therapy. *FEBS J*. (2021) doi: 10.1111/febs.15739. [Epub ahead of print].
167. Narayana A, Kunnakkat S, Chacko-Mathew J, Gardner S, Karajannis M, Raza S, et al. Bevacizumab in recurrent high-grade pediatric gliomas. *Neuro Oncol*. (2010) 12:985–90. doi: 10.1093/neuonc/noon033
168. Lin F, de Gooijer MC, Hanekamp D, Chandrasekaran G, Buil LCM, Thota N, et al. PI3K-mTOR pathway inhibition exhibits efficacy against high-grade glioma in clinically relevant mouse models. *Clin Cancer Res*. (2017) 23:1286–98. doi: 10.1158/1078-0432.CCR-16-1276
169. Robinson GW, Orr BA, Gajjar A. Complete clinical regression of a BRAF V600E-mutant pediatric glioblastoma multiforme after BRAF inhibitor therapy. *BMC Cancer*. (2014) 14:258. doi: 10.1186/1471-2407-14-258
170. Zhao X, Kotch C, Fox E, Surrey LF, Wertheim GB, Baloch ZW, et al. NTRK fusions identified in pediatric tumors: the frequency, fusion partners, and clinical outcome. *JCO Precis Oncol*. (2021) 1:PO.20.00250. doi: 10.1200/PO.20.00250
171. Huang SY, Yang J-Y. Targeting the hedgehog pathway in pediatric medulloblastoma. *Cancers*. (2015) 7:2110–23. doi: 10.3390/cancers7040880
172. Long W, Yi Y, Chen S, Cao Q, Zhao W, Liu Q. Potential new therapies for pediatric diffuse intrinsic pontine glioma. *Front Pharmacol*. (2017) 8:495. doi: 10.3389/fphar.2017.00495
173. Sadelain M, Brentjens R, Rivière I. The basic principles of chimeric antigen receptor design. *Cancer Discov*. (2013) 3:388–98. doi: 10.1158/2159-8290.CD-12-0548
174. van der Stegen SJC, Hamieh M, Sadelain M. The pharmacology of second-generation chimeric antigen receptors. *Nat Rev Drug Discov*. (2015) 14:499–509. doi: 10.1038/nrd4597
175. June CH, Sadelain M. Chimeric antigen receptor therapy. *N Engl J Med*. (2018) 379:64–73. doi: 10.1056/NEJMra1706169
176. Patterson JD, Henson JC, Breese RO, Bielamowicz KJ, Rodriguez A. CAR T Cell therapy for pediatric brain tumors. *Front Oncol*. (2020) 10:1582. doi: 10.3389/fonc.2020.01582
177. Gaudino SJ, Kumar P. Cross-talk between antigen presenting cells and T cells impacts intestinal homeostasis, bacterial infections, and tumorigenesis. *Front Immunol*. (2019) 10:360. doi: 10.3389/fimmu.2019.00360
178. Akhavan D, Alizadeh D, Wang D, Weist MR, Shepphird JK, Brown CE. CAR T cells for brain tumors: lessons learned and road ahead. *Immunol Rev*. (2019) 290:60–84. doi: 10.1111/imr.12773
179. Vitanza NA, Johnson AJ, Wilson AL, Brown C, Yokoyama JK, Künkele A, et al. Locoregional infusion of HER2-specific CAR T cells in children and young adults with recurrent or refractory CNS tumors: an interim analysis. *Nat Med*. (2021) 27:1544–52. doi: 10.1038/s41591-021-01404-8
180. Kabir TF, Chauhan A, Anthony L, Hildebrandt GC. Immune checkpoint inhibitors in pediatric solid tumors: status in 2018. *Ochsner J*. (2018) 18:370–6. doi: 10.31486/toj.18.0055
181. Peggs KS, Quezada SA, Allison JP. Cell intrinsic mechanisms of T-cell inhibition and application to cancer therapy. *Immunol Rev*. (2008) 224:141–65. doi: 10.1111/j.1600-065X.2008.00649.x
182. Park JA, Cheung N-KV. Limitations and opportunities for immune checkpoint inhibitors in pediatric malignancies. *Cancer Treat Rev*. (2017) 58:22–33. doi: 10.1016/j.ctrv.2017.05.006
183. Wherry EJ, Kurachi M. Molecular and cellular insights into T cell exhaustion. *Nat Rev Immunol*. (2015) 15:486–99. doi: 10.1038/nri3862

184. Wintterle S, Schreiner B, Mitsdoerffer M, Schneider D, Chen L, Meyermann R, et al. Expression of the B7-related molecule B7-H1 by glioma cells. *Cancer Res.* (2003) 63:7462–7.
185. Yao Y, Tao R, Wang X, Wang Y, Mao Y, Zhou LF. B7-H1 is correlated with malignancy-grade gliomas but is not expressed exclusively on tumor stem-like cells. *Neuro Oncol.* (2009) 11:757–66. doi: 10.1215/15228517-2009-014
186. Gorski HS, Malicki DM, Barsan V, Tumblin M, Yeh-Nayre L, Millburn M, et al. Nivolumab in the treatment of recurrent or refractory pediatric brain tumors: a single institutional experience. *J Pediatr Hematol Oncol.* (2019) 41:e235–41. doi: 10.1097/MPH.0000000000001339
187. Cacciotti C, Choi J, Alexandrescu S, Zimmerman MA, Cooney TM, Chordas C, et al. Immune checkpoint inhibition for pediatric patients with recurrent/refractory CNS tumors: a single institution experience. *J Neurooncol.* (2020) 149:113–22. doi: 10.1007/s11060-020-03578-6
188. Wang SS, Bandopadhyay P, Jenkins MR. Towards immunotherapy for pediatric brain tumors. *Trends Immunol.* (2019) 40:748–61. doi: 10.1016/j.it.2019.05.009
189. Soldozy S, Skaff A, Soldozy K, Sokolowski JD, Norat P, Yagmurli K, et al. From bench to bedside, the current state of oncolytic virotherapy in pediatric glioma. *Neurosurgery.* (2020) 87:1091–7. doi: 10.1093/neuros/nyaa247
190. Lun XQ, Zhou H, Alain T, Sun B, Wang L, Barrett JW, et al. Targeting human medulloblastoma: oncolytic virotherapy with myxoma virus is enhanced by rapamycin. *Cancer Res.* (2007) 67:8818–27. doi: 10.1158/0008-5472.CAN-07-1214
191. Wu Y, Lun X, Zhou H, Wang L, Sun B, Bell JC, et al. Oncolytic efficacy of recombinant vesicular stomatitis virus and myxoma virus in experimental models of rhabdoid tumors. *Clin Cancer Res.* (2008) 14:1218–27. doi: 10.1158/1078-0432.CCR-07-1330
192. Ashley DM, Thompson EM, Landi D, Desjardins A, Friedman AH, Threatt S, et al. HGG-22. phase 1b study polio vaccine sabin-rhinovirus poliovirus (PVSRIPO) for recurrent malignant glioma in children. *Neuro Oncol.* (2018) 20:i93. doi: 10.1093/neuonc/ny059.294
193. Gromeier M, Nair SK. Recombinant poliovirus for cancer immunotherapy. *Annu Rev Med.* (2018) 69:289–99. doi: 10.1146/annurev-med-050715-104655
194. Tejada S, Alonso M, Patiño A, Fueyo J, Gomez-Manzano C, Diez-Valle R. Phase I trial of DNX-2401 for diffuse intrinsic pontine glioma newly diagnosed in pediatric patients. *Neurosurgery.* (2018) 83:1050–6. doi: 10.1093/neuros/nyx507
195. Liu Z, Zhao X, Mao H, Baxter PA, Huang Y, Yu L, et al. Intravenous injection of oncolytic picornavirus SVV-001 prolongs animal survival in a panel of primary tumor-based orthotopic xenograft mouse models of pediatric glioma. *Neuro Oncol.* (2013) 15:1173–85. doi: 10.1093/neuonc/not065
196. Landi DB, Thompson EM, Ashley DM. Immunotherapy for pediatric brain tumors. *Neuroimmunol Neuroinflamm.* (2018) 5:29. doi: 10.20517/2347-8659.2018.35
197. Friedman GK, Johnston JM, Bag AK, Bernstock JD, Li R, Aban I, et al. Oncolytic HSV-1 G207 immunovirotherapy for pediatric high-grade gliomas. *N Engl J Med.* (2021) 384:1613–22. doi: 10.1056/NEJMoa2024947
198. Varela-Guruceaga M, Tejada-Solis S, García-Moure M, Fueyo J, Gomez-Manzano C, Patiño-García A, et al. Oncolytic viruses as therapeutic tools for pediatric brain tumors. *Cancers.* (2018) 10:226. doi: 10.3390/cancers10070226
199. Ochs K, Ott M, Bunse T, Sahm F, Bunse L, Deumelandt K, et al. K27M-mutant histone-3 as a novel target for glioma immunotherapy. *Oncoimmunology.* (2017) 6:e1328340. doi: 10.1080/2162402X.2017.1328340
200. Schaller TH, Sampson JH. Advances and challenges: dendritic cell vaccination strategies for glioblastoma. *Expert Rev Vaccines.* (2017) 16:27–36. doi: 10.1080/14760584.2016.1218762
201. Banchereau J, Palucka K. Immunotherapy: cancer vaccines on the move. *Nat Rev Clin Oncol.* (2018) 15:9–10. doi: 10.1038/nrclinonc.2017.149
202. Rutkowski S, De Vleeschouwer S, Kaempgen E, Wolff JEA, Kühl J, Demaerel P, et al. Surgery and adjuvant dendritic cell-based tumour vaccination for patients with relapsed malignant glioma, a feasibility study. *Br J Cancer.* (2004) 91:1656–62. doi: 10.1038/sj.bjc.6602195
203. De Vleeschouwer S, Fieus S, Rutkowski S, Van Calenbergh F, Van Loon J, Goffin J, et al. Postoperative adjuvant dendritic cell-based immunotherapy in patients with relapsed glioblastoma multiforme. *Clin Cancer Res.* (2008) 14:3098–104. doi: 10.1158/1078-0432.CCR-07-4875
204. Faury D, Nantel A, Dunn SE, Guiot M-C, Haque T, Hauser P, et al. Molecular profiling identifies prognostic subgroups of pediatric glioblastoma and shows increased YB-1 expression in tumors. *J Clin Oncol.* (2007) 25:1196–208. doi: 10.1200/JCO.2006.07.8626

Conflict of Interest: The authors declare that the research was conducted in the absence of any commercial or financial relationships that could be construed as a potential conflict of interest.

Publisher's Note: All claims expressed in this article are solely those of the authors and do not necessarily represent those of their affiliated organizations, or those of the publisher, the editors and the reviewers. Any product that may be evaluated in this article, or claim that may be made by its manufacturer, is not guaranteed or endorsed by the publisher.

Copyright © 2021 Gonçalves, Viaene and Vossough. This is an open-access article distributed under the terms of the Creative Commons Attribution License (CC BY). The use, distribution or reproduction in other forums is permitted, provided the original author(s) and the copyright owner(s) are credited and that the original publication in this journal is cited, in accordance with accepted academic practice. No use, distribution or reproduction is permitted which does not comply with these terms.